Archives of Biochemistry and Biophysics 596 (2016) 22–42

Contents lists available at ScienceDirect

Archives of Biochemistry and Biophysics

journal homepage: www.elsevier.com/locate/yabbi

Review article

A review of solute encapsulating nanoparticles used as delivery systems with emphasis on branched amphipathic peptide capsules

Sheila M. Barros [a, b], Susan K. Whitaker [a], Pinakin Sukthankar [a, 1], L. Adriana Avila [a, 2], Sushanth Gudlur [a, 3], Matt Warner [a], Eduardo I.C. Beltrão [b], John M. Tomich [a, *]

[a] Department of Biochemistry and Molecular Biophysics, Kansas State University, Manhattan, KS 66506, USA
[b] Department of Biochemistry, Federal University of Pernambuco-UFPE, Recife, Pernambuco, 50670-901, Brazil

ARTICLE INFO

Article history:
Received 5 November 2015
Received in revised form
24 February 2016
Accepted 26 February 2016
Available online 27 February 2016

Keywords:
BAPCs
Nanoparticle
Drug delivery
Self-assembly
Peptide bilayer

ABSTRACT

Various strategies are being developed to improve delivery and increase the biological half-lives of pharmacological agents. To address these issues, drug delivery technologies rely on different nano-sized molecules including: lipid vesicles, viral capsids and nano-particles. Peptides are a constituent of many of these nanomaterials and overcome some limitations associated with lipid-based or viral delivery systems, such as tune-ability, stability, specificity, inflammation, and antigenicity. This review focuses on the evolution of bio-based drug delivery nanomaterials that self-assemble forming vesicles/capsules. While lipid vesicles are preeminent among the structures; peptide-based constructs are emerging, in particular peptide bilayer delimited capsules.

The novel biomaterial—Branched Amphiphilic Peptide Capsules (BAPCs) display many desirable properties. These nano-spheres are comprised of two branched peptides—bis(FLIVI)-K-KKKK and bis(FLIVIGSII)-K-KKKK, designed to mimic diacyl-phosphoglycerides in molecular architecture. They undergo supramolecular self-assembly and form solvent-filled, bilayer delineated capsules with sizes ranging from 20 nm to 2 μm depending on annealing temperatures and time. They are able to encapsulate different fluorescent dyes, therapeutic drugs, radionuclides and even small proteins. While sharing many properties with lipid vesicles, the BAPCs are much more robust. They have been analyzed for stability, size, cellular uptake and localization, intra-cellular retention and, bio-distribution both in culture and in vivo.

Contents

* Corresponding author. Department of Biochemistry and Molecular Biophysics, 141 Chalmers Hall, Kansas State University, Manhattan, KS, 66506, USA.
E-mail address: jtomich@ksu.edu (J.M. Tomich).
[1] Current address: Department of Molecular Biosciences, University of Kansas, Lawrence KS 66045, USA.
[2] Current address: Department of Chemistry and Biochemistry, Auburn University Auburn AL 36849, USA.
[3] Current address: Center for Biomimetic Sensor Science (CBSS) Nanyang Technological University, 637553 Singapore.

http://dx.doi.org/10.1016/j.abb.2016.02.027
0003-9861/

1. Introduction

A goal of pharmaceutical research is to deliver drugs at appropriate dosages to target cells or tissues in a safe and reproducible manner [1]. While tremendous progress has been made in defining fundamental biological processes and discovering compounds that interact with these molecules, translation of these findings into advanced therapies has lagged behind. Limitations in delivering therapeutic moieties to selective tissues with minimal off-target damage are often cited for this lapse [1,2]. Novel molecular pharmacological agents with proven biological activities but limited aqueous solubilities or short circulating half-lives in vivo will face substantive barriers. These delivery impediments limit or reduce therapeutic activity and disfavor potential pharmaceutically interesting compounds from entering clinical drug trials [1]. Conventional modes of drug administration such as pills, eye drops, intravenous solutions, ointments, inhalers etc., fall short in meeting these expectations. The oral route for example is one of the most commonly employed and preferred modes for drug administration due to its minimally invasive nature. However the adequate delivery of peptide and protein drug candidates fuelled by the recent advances in recombinant biotechnology [2], are ineffective via this route [3,4]. Overcoming numerous barriers including—the acid environment of the human stomach, proteolytic degradation, limited intestinal uptake and first pass effects of the liver is essential. All of these factors reduce, alter and block absorption of almost all biomacromolecular therapeutics [5,6].

Self-assembling nano-carriers (Fig. 1) show promise as delivery vehicles that overcome many of the poor absorption issues that plague certain classes of drugs. Both hydrophobic and hydrophilic small molecules, proteins, and nucleic acids can be bound to or encapsulated within the compartments of these nanomaterials and delivered in vitro or in vivo. The self-assembling carriers can be classified into a number of categories depending on whether they are solid or hollow and the materials that comprise them. They can be further categorized depending on whether they contain natural or synthetic polymers. Polymeric vesicles offer advantages over their natural counterparts (Liposomes) in terms of stability, storage and tune-ability. Drug delivery through polymeric vesicles increases the stability of the drug, extends the circulating time in the bloodstream and can be designed for controlled release. Most polymersomes and peptide amphiphiles have low “critical assembly concentrations” (CAC), a value similar to the critical micelle concentration (CMC), used to describe the minimum concentration needed to form lipid vesicles. Their CAC's fall in the range of 10^{-6} – 10^{-7} M, which is 1000 times lower than most surfactants (10^{-3} – 10^{-4} M) [7,8]. This allows for the retention of payloads for longer periods as well as improved delivery to distal areas of the body. A review of the literature reveals a plethora of compounds encapsulated and successfully delivered in vitro and in vivo using polymeric vesicles. These include various anti-cancer drugs like Doxorubicin and Paclitaxel, proteins like myoglobin, hemoglobin and albumin, fluorescent molecules, plasmids and siRNA. The review by Levine et al. (2008) [9] summarizes the literature on polymersome research related to cancer diagnosis and therapeutics, giving a more detailed account of the types of polymersomes and cargo that have been developed to that point.

Polymeric vesicles are also useful as diagnostic tools and in optical imaging when they encapsulate fluorescent agents. One example is the encapsulation of a porphyrin-based near infrared (NIR) fluorophore that is able to generate a signal even through a 1 cm solid tumor [10]. When such nanovesicles are injected into an animal, their biodistribution can be monitored using non-invasive NIR optical methods eliminating the need to sacrifice the animal.

The surface of these nanovesicles can be functionalized with various ligand molecules specific for up-regulated surface receptors on diseased cells. Such site-specific delivery reduces potential systemic side-effects observed using traditional delivery routes. Some of the ligand molecules attempted include various antibodies, transactivator of transcription (TAT) peptide and anti-HER-2/neu *peptide* mimetic (AHNP) peptides.

Nano-vectors have been shown to improve the pharmacological characteristics of these drug moieties. The utilization of nanotechnology for drug delivery has been shown to enhance the delivery of poorly soluble drugs, facilitate drug targeting in a cell/tissue-specific manner and enabled the co-delivery of two or more drugs as well the intracellular delivery of larger macromolecular drugs. By enhancing the efficacy of these drugs, new candidate drugs are advancing in clinical trials with improved safety and effectiveness [11]. The application of nanotechnology to drug delivery is expected to alter the landscape of pharmaceutical and biotechnology industries in the foreseeable future [11–14]. As of 2013, almost 250 nanotechnology based medicines had been approved or were in various stages of clinical investigation [15–17].

Nanoparticulates are colloidal macromolecular nanocarrier systems ranging from 10 to 200 nm and deemed as potentially

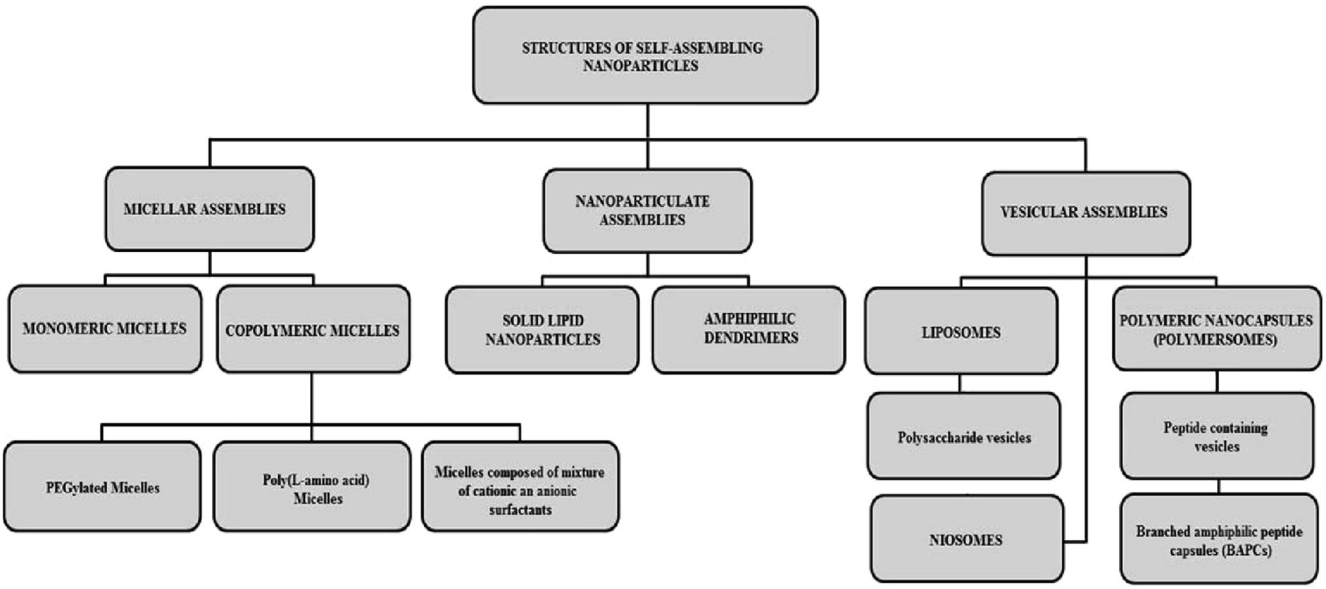

Fig. 1. Classification of nanocarrier systems for drug delivery.

attractive candidates for the entrapment and encapsulation of hydrophobic drugs. Solid nanoparticulates can either be defined as nanocapsules - where the active drug molecule is encapsulated within the carrier; or matrix based nanospheres - where the drug molecules are adsorbed and dispersed throughout the nanomaterial [18]. Nanoparticulates can be engineered using 'top down' or 'bottom up' methods [19]. In the former, a larger material is broken down into smaller particles whereas the bottom up approach involves the thermodynamically regulated, multi-step synthesis of the nanomaterial in a controlled reaction [20].

A competent nano-carrier functions safely, selectively, reliably delivering a therapeutic at the required dosage to the target site in the appropriate time frame [3,13,20,21]. Ideal nano-carriers possess several desirable attributes: they should reduce the concentrations of the active compound needed since the drugs are no longer systemically distributed [22] and the pharmacokinetics of biodistribution are enhanced due to improved tissues and organ targeting [12,23–25]. This preferential delivery along with the particle's ability to release drugs in a sustained or stimuli triggered manner will reduce off-target effects and decrease cytotoxicity. Utilization of nano-carriers has the added advantage of improving the delivery of hydrophobic drugs in water; thus enhancing their delivery through parenteral administration. Nano-carrier based delivery systems have also been shown to improve the half-lives of a wide variety of hydrophobic moieties and peptide drugs [26–28]. Moreover, nanotechnology based delivery vehicles composed of biocompatible molecules [29–32] are projected as safer alternatives to existing vehicles that have been known to cause peripheral neuropathy and hypersensitivity [33,34].

The search for nano-delivery systems involves numerous design elements. The large repertoire of available nano-carriers, apart the ones that are in development, present nano-systems with a variety of structural, functional and physiochemical characteristics that translate into case specific advantages and/or limitations. These include (i) biocompatibility of constituent material(s); (ii) simple and robust assembly processes; (iii) functionalization/pre-functionalization capability; (iv) intracellular stability and biodegradability; (v) long circulating half-life; (vi) a size compatible with facile cellular uptake, charge density, surface hydrophilicity and flexibility; and (vii) negligible immunogenicity.

It has been indicated that the complexity involved in nanoparticle fabrication and functionalization causes batch to batch variations leading to quality and purity concerns [3]. The development of targeted nano-carriers via a single step synthesis mediated by the self-assembly of pre-functionalized biomaterials would serve to alleviate these concerns by simplifying the optimization and the scalable manufacture of these systems [35–38].

Despite recent advancements in nano-medicine, several challenges remain – 1) over-coming physicochemical and biological hurdles such as low stability, low permeability, short half-life, enzymatic susceptibility, targeting and 2) immunogenicity [5]. Although a majority of these nano-therapeutic products have improved the pharmaceutical efficacy of clinically approved drugs, nanotechnology as a whole has not yet generated entirely new therapies [11].

2. Structures of self-assembling nanoparticles

The phenomenon of bio-molecular self-assembly is a common in nature. Assembled multi-protein complexes are required for a number of cellular functions. Diacylglycerol-phospholipid assembly is responsible for the structure of the various cell membranes. In the context of lipids and peptides, the self-assembling molecules are amphiphilic and are comprised of both hydrophobic and hydrophilic domains. These domains can be spatially separated either along the length of the molecule or along a defined face of the folded molecule [39]. The hydrophilic segments can either be uncharged (polar) or charged (cationic, anionic or zwitterionic) [40]. While such segments are spatially segregated in lipids, in amphipathic peptides the primary sequences contain alternating or random segments of hydrophobic and hydrophilic residues. Upon folding into either helices or β-sheets, the final functional structures have continuous faces of hydrophobic or hydrophilic residues that allow them to interact with solvent, a membrane, a ligand or an adjacent molecule.

Self-assembly in bio-macromolecules is usually facilitated by weak non-covalent interactions that can be any one or a mixture of hydrogen bonding, Van der Waal forces, ionic, and electrostatic interactions. When such amphiphilic molecules are introduced into an aqueous environment, the hydrophobic segments anneal to

exclude water thereby providing the driving force for assembly aided by inter- and intra-molecular associations. The hydrophilic segments of the molecule remain exposed to the aqueous solvent. Much of our understanding of self-assembly of amphiphiles comes from studies with lipids. Attempts to mimic lipid amphiphiles have led to the design and development of many different types of molecules that retain the amphiphilic character with relatively short acyl-chains [41,42].

Lipid and peptide amphiphiles assemble into a number of nano- and micro-sized structures such as micelles, vesicles or molecular gels [43] composed of rods and tubules [44], fibrils and fibers [45] with ordered structures. Micelles adopt spherical, worm like or disk shaped structures [46–51]. Vesicles when composed entirely of lipids are called liposomes, but other non-lipid vesicle types exist: niosomes, proniosomes, polyhedral niosomes, polymersomes and vesicles formed by the self-assembly of peptide amphiphiles (peptosomes) [52]. Finally, structures that do not fall into either of these common categories can be as diverse as, bipyramids, lamellar, hexagonal phase, cubic phase, icosahedral, cage like, high axial ratio microstructures (HARM) [53–55] and myelin fibrils [40]. The energetics, geometric constraints and strengths of the intra- and inter-interacting forces of the individual molecules determine the final architecture of the assembly. Other factors influencing the final assembly are pH, temperature, ionic strength of the solvent, as well as the concentration of the monomer. Using the packing parameter of the monomer one can predict the favored structure of the assembly [56]. The packing parameter depends on the area of the head group a_0, molal volume of the hydrocarbon chain or chains v, and the extended chain length l_0 of the monomer:

$$\text{Packing number} = \frac{v}{a_0 l_0}$$

While the head group of the amphiphiles plays a critical role in predicting the overall shape and size of the assemblies, the tail region directs the formation of spherical micelles, rod like micelles and spherical bilayer vesicles [43]. While there are numerous review articles focused on the different morphologies adopted by self-assembling molecules, this review is concerned with studies on spherical aggregates, namely micelles and vesicles.

2.1. Micellar assemblies

2.1.1. Monomeric micelles

Micelles are the simplest amphiphilic assembly. They are useful in encapsulating hydrophobic molecules within their hydrophobic core (Fig. 2).

Detergent micelles comprised of sulfated acyl chains (i.e. sodium dodecyl sulfate, SDS) adopt this structure. At concentrations below their CMC, the amphiphiles exist as monomers but as the monomer concentration exceeds the CMC, they begin to assemble into stable spherical structures. These structures are in a dynamic equilibrium with the monomers present in solution. The CMC is affected by further increases in concentration of the amphiphile that can lead to a change in the overall shape (discoidal, rod like or liquid crystalline phase), thus allowing one to tune the overall shape and size of the final assembly. Lipid micelles range from 10 to 100 nm in diameter and exhibit a core-shell architecture, in which the interior, being hydrophobic, entraps lipophilic drugs [57]. The CMC and structural features exhibited by micelles are a function of the nature of their hydrophilic and hydrophobic block constituents. Yu and Eisenberg [58] generated a variety of micellar conformers such as, spheres, rods, vesicles, tubules and lamellae depending on solvent conditions and the relative size of hydrophobic and hydrophilic segments. These different structures when tested for their ability to deliver drugs displayed varied pharmacokinetic properties. [59–63].

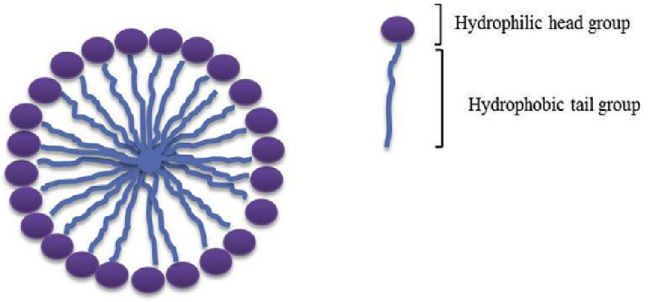

Fig. 2. Illustration of a micelle.

2.1.2. Copolymeric micelles

Copolymeric micelles are relatively new constructs that incorporate biodegradable polymers prepared from block copolymers. Block copolymers are linear repeating units of hydrophobic and hydrophilic residues covalently linked to impart amphilicity to the molecule. $K_{60}L_{20}$ is one such example of a diblock copolymer where a polypeptide comprised of sixty lysine residues is covalently linked to a polypeptide composed of twenty leucine residues. The block of leucine residues form the hydrophobic segment of the block copolymer while the positively charged lysine residues form the more hydrophilic segment [64]. Triblock copolymers are similar to diblock copolymers but differ in having an extra hydrophobic or hydrophilic segment that can be fused to either of the existing segments. In general, a polymeric micelle consists of two parts: a core shell composed of insoluble hydrophobic segments and the outer corona composed of the soluble hydrophilic segments (Fig. 3). While simple spherical micelles with a core particle and corona are common, more complex multi-lamellar structures have been recently reported that resemble onion-like micelles [65], shell cross-linked micelles [66], star shaped Janus micelles that allow for two different types of chemical interactions in the same molecule [67–69] schizophrenic diblock copolymer micelles [70], multi-compartmental hamburger micelles [71].

2.1.2.1. PEGylated micelles. Numerous copolymers have been used to produce micelles, but biocompatibility and biodegradability issues have limited their use in therapeutic applications [72]. Usually, the preferred choice for the hydrophilic block has been polyethylene glycol (PEG). In most micellar assemblies, the molecular weight of PEG tends to exceed that of the hydrophobic core-forming block [73]. This outer hydrophilic corona region tends to

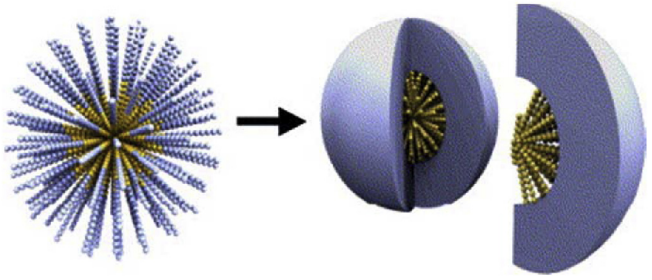

Fig. 3. Polymeric micelle. Self-assembly and polymerization of a block copolymers yielda shell cross-linked knedel polymer assemblies, where the cross-linked outer shell can be decorated with biologically relevant ligands. [Reprinted from *Adv Drug Deliv. Rev*, 56(11), Tu and Tirrell, Bottom-up design of biomimetic assemblies, 1537–1563 (2004) [42] with permission from Elsevier].

become hydrated resulting in a splayed appearance, giving rise to various structures, such as polymer brushes [74]. These conformations imbue the micelles with new properties that suppress binding of serum proteins and phagocytic attack in blood thereby decreasing clearance by the reticuloendothelial system (RES) [75]. PEGylated co-polymer micelles also have lower CAC's than traditional surfactants resulting in reduced cytotoxicity [76]. The highly hydrated corona and the hydrophobic core generate a dielectric gradient that aids in the solubilization of a range of non-polar compounds of varied hydrophobicities [77]. Micellar delivery systems, like many other ones, positively affect the biodistribution and pharmacokinetics of drugs by means of increased circulating half-lives and increased tumor accumulation [78].

2.1.2.2. Poly(L-amino acid) micelles. Poly(L-amino acid) micelles are formed from poly(L-Histidine)-PEG block co-polymers combined with poly(L-lactic acid)-PEG (PLLA-PEG). These micelles have been investigated as pH sensitive drug carriers for cancer therapy [79–81]. Cancerous cells - due to a higher rate of metabolism - tends to have intracellular pH values < 7.2 [82–84]. The imidazole side-chain of histidine has a pKa in this range; which leads to an increase in histidine hydrophobicity, destabilization of the micelle and subsequent drug release. The pH sensitivity of Poly(L-amino acid) micelles can be modulated by varying the %wt. of the poly(L-lactic acid)-PEG composition. Moreover, Poly(L-histidine) (PLHS) appears to have fusogenic activity with endosomes facilitating cytosolic drug release in cancer cells. More complex systems that incorporate phenylalanine ([poly(His-co-Phe)]-PEG) and 1,2-distearoyl-sn-glycero-3-phosphoethanolamine-polyethylene glycol-2000(DSPE-PEG) have recently been formulated to decrease the pH sensitivity of the pure poly L-histidine and also act as pH sensitive nanocarriers for cytosolic drug delivery [85]. Drugs have been conjugated to these poly(amino acid) copolymers via chemical modifications of the drugs, but not without concerns relating to drug decoupling at the target site [86–88]. Also, immunogenicity is a potential concern with these systems upon the increase in the number and diversity of amino acids used [71].

2.1.2.3. Micelles composed of mixtures of cationic and anionic surfactants. The preparation of micelles using two surfactants of opposite net charge is well established [89–91]. Charge repulsion of the head groups decreases the free energy of assembly [92]. The size and net charge of the detergent pair determines the CMC as well as the size of the resulting micelles [93]. In a single report the mixing of certain oppositely charged surfactants can lead to the spontaneous formation of single walled vesicles [94]. The size, charge and permeability of such vesicles was controlled by adjusting the molar ratios of the two surfactants. One example of such a charge balancing mixture is cetyl trimethylammonium tosylate (CTAT) and sodium dodecylbenzene sulfonate (SDBS).

2.2. Nanoparticulate assemblies

2.2.1. Solid lipid nanoparticles

Solid Lipid Nanoparticles (SLNs) are members of a class of nanoscale carriers consisting of a central solid hydrophobic core comprised of physiological lipids emulsified with an aqueous surfactant [95]. Hydrophobic drugs are dissolved in the solid hydrophobic core [96]. These nanoparticles due to their narrow size range (100–200 nm) evade the RES and cross the blood-brain barrier [97]. The biodegradable properties of these lipids minimize their cytotoxicity. SLNs also demonstrate stable drug entrapment, especially in case of very hydrophobic drugs and provide controlled release lasting several weeks. SLN can be conjugated to hydrophilic polymers and/or surfactants to minimize their hepatic uptake and improve bioavailability [58]. SLNs can be stabilized with stearic acid - PEG 2000, however cytotoxic effects have been observed upon the release of free stearic acid [98]. By choosing lipids with varying chain lengths and degrees of unsaturation the loading capacity of SLNs can be controlled. Overall, SLNs appear to be safe delivery systems for hydrophobic drugs especially to the brain and production is scalable with excellent reproducibility [99,100].

2.2.2. Amphiphilic dendrimers

Dendrimers are 1–10 nm sized hyper-branched synthetic polymers comprised of well-defined branched oligomers attached to a central core [101–103]. Dendrimers are synthesized using convergent or divergent approaches [103]. The former approach capitalizes on the symmetric nature of the dendrimer with synthesis commencing at the periphery and terminating at the core; while the divergent approaches builds out from the core [104]. Dendrimers display low poly-dispersity despite their large molecular mass. The branching of the dendrimers generates semi-globular/globular structures that are easily functionalized [103]. Glycol-, peptide- and silicon-capped dendrimers have been synthesized using carbohydrates, peptides and silicon [39,105]. Drugs can associate with dendrimers through physical entrapment within the void spaces or by attachment of the pro-drug to functional groups positioned on the dendrimer surface [94].

Amphiphilic dendrimers (Janus dendrimers) are capable of self-assembling into stable bilayer vesicles, referred to as dendrimersomes [106]. A Janus dendrimer is formed by covalently linking two distinct dendritic building blocks. They can be made amphiphilic by attaching a non-polar block (e.g. alkoxy gallate ether to a polar block such as aliphatic arborol) [107]. A review by Rosen et al. (2009) [108] details the self-assembly and disassembly

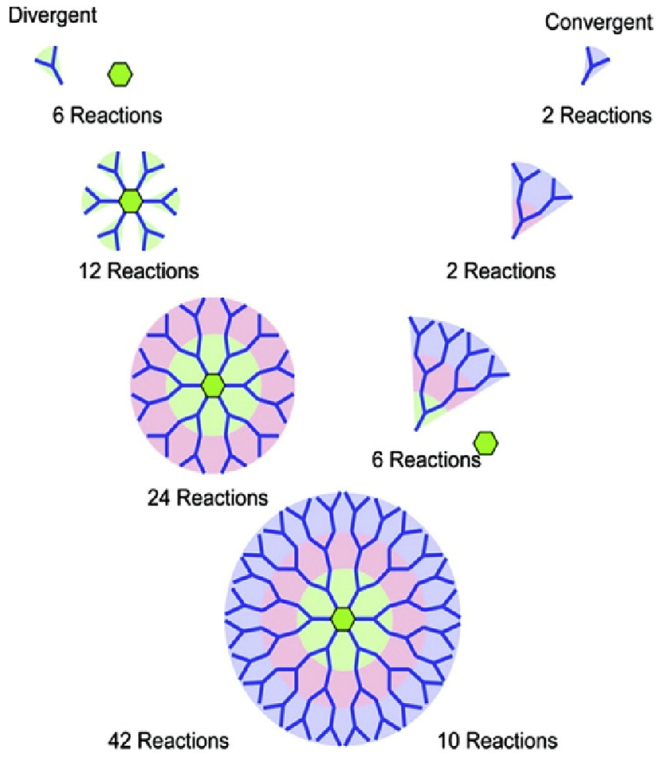

Fig. 4. Convergent and divergent synthesis of dendrimers and dendrons. Reprinted (adapted) with permission from Rosen et al. (2009) [108], Chem Rev., **109**(11), 6275–6540. Copyright 2009 American Chemical Society.

of dendrons. Fig. 4, is an illustration reproduced from the above review.

Dendrimers have been studied for the delivery of fluorouracil [109] and indomethacin [110]. Dendrimer size has been exponentially correlated with the duration of extravasation across the endothelium, with larger dendrimers indicating faster extravasations [111]. The positive charges on the polyamine and/or polyamide linkages used in some dendrimers pose a potential risk for cellular toxicity and immune activation. Partial derivatization of the dendrimer surface with PEG and/or fatty acids is known to mitigate these concerns by shielding the positive charges on the surface [112,113].

2.3. Vesicular assemblies

In contrast to the different micellar constructs discussed above where drugs are trapped within the micellar matrix, the ability of vesicles to encapsulate solutes offers increased versatility. Their hollow interiors permit encapsulation of higher concentrations of cargo, thus making them potentially better drug delivering vehicles. Vesicles are colloidal aggregates that are most often spherical. In biology, lipid vesicles are bilayer-delimited chambers that entrap solvent during the self-assembly process. The solvent is water containing dissolved solutes. In terms of drug delivery, solutes including peptides, proteins, genetic material, or bioactive compounds like anticancer drugs can be encapsulated. It can also trap non-polar or hydrophobic substances within their membrane, thereby increasing their utility. Such versatility has made them the most attractive choice for use in biology. Apart from its biological/medical uses, vesicles can be used as micro-chemical reactors and have found application in the cosmetic and food industries [114]. Lipid based vesicles are the most extensively studied drug carriers used today. Until recently, lipids were the only choice for generating artificial vesicles. However with the introduction of many new self-assembling molecules, one can choose from a variety of molecules. Figure 1, classifies the various polymeric vesicles described to date. It is difficult to precisely classify all of the various polymeric vesicles due to the issue of multi-functionality. This is particularly true with the introduction of hybrid polymers, where two or more different materials are used to make an amphiphile such as combining the synthetic polymer polyethylene oxide (PEO) to either a polypeptide or a diacylglycerol phospholipid. These hybrid polymers can improve solubility, increase circulating half-lives in the bloodstream and allow for the surface functionalizing with desired targeting ligands. Such a molecule could be classified as a block.

Copolymer, lipid vesicle or peptide vesicle depending on the proportions of the individual components and/or which component is driving the assembly [103]. Employing natural biopolymer vesicles as drug carriers over synthetic and semi-synthetic polymer vesicles improves their biocompatible and biodegradable. Lipids, polysaccharides and peptides are all capable of self-assembling into vesicles and other nano- and micro-sized structures [115].

2.3.1. Liposomes

Liposomes or lipid vesicles are possibly the oldest and most widely studied drug delivery systems and have been in use since the 1960s [116,117]. These artificially produced vesicles range from 30 nm to several micrometers in size and consist of an aqueous core surrounded by uni- or multi-lamellar membranes formed from the supramolecular-assembly of primarily phospholipids (Fig. 5) and cholesterol. Numerous studies have promoted the use of these structures [118–120].

Liposomes can be prepared from a variety of diacyl phospholipids including: 1,2-Dimyristoyl-*sn*-glycero-3-phosphocholine (DMPC), 1,2 Dipalmitoyl-sn-glycero-3-choline (DPPC), and 1-palmitoyl-2-oleoyl-sn-glycero-3-phosphocholine (POPC), palmitoyl-2-oleoylphosphatidylethanolamine (POPE) among others. As an example we show POPC:POPE vesicles generated in our laboratory as well as their resizing after extrusion (Fig.6). Most of our knowledge on vesicle assembly, dynamics and physical properties come from studies on these assemblies. Since then, many different and diverse vesicles have been designed and developed. Unlike polypeptides and polysaccharides, lipids are not polymers. Liposomes have found uses in many biological, pharmaceutical and cosmetic applications. They are employed in studies related to cell physiology, as model cell membranes and drug delivery vehicles.

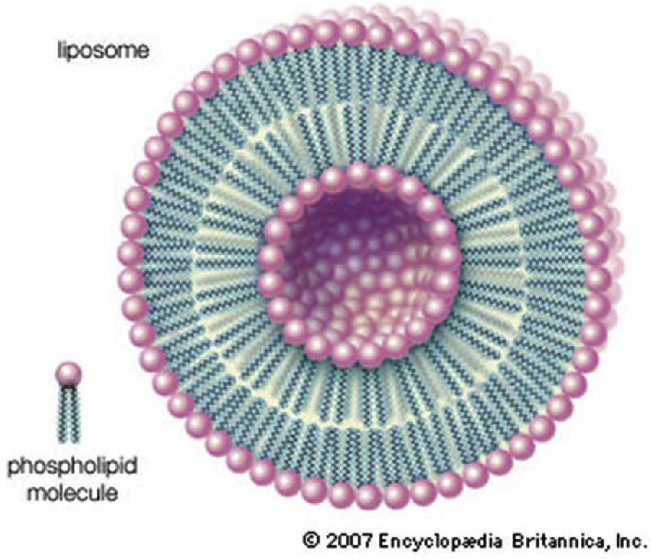

Fig. 5. Illustration of a Liposome. By courtesy of Encyclopaedia Britannica, Inc., copyright 2007; used with permission. [http://www.britannica.com/EBchecked/media/92244/Phospholipids-can-be-used-to-form-artificial-structures-called-liposomes].

Their utility lies in their ability to fuse with cellular membranes [121] and lipid bilayers membranes or enter cells through clathrin-mediated endocytosis [122,123]. The properties of liposomes have been modulated to produce variation in size, lipid composition, surface charge and other characteristics [77]. The aqueous core of the liposomes is known to encapsulate large payloads of hydrophilic and moderately hydrophobic drugs; and their ability to naturally associate with tumors and the EPR effect has led to the development of numerous FDA approved drugs based on the liposome platform [72,100,124].

Numerous studies have been conducted to surface modify classical liposomes in an effort to increase their targeting capabilities and circulating half-lives. These include the introduction of linear dextrans [125], gangliosides containing sialic acid [126], lipid derivatives of hydrophilic polymers such as polyvinyl alcohol [127], polyethylene glycol [128,129] and poly-N-vinylpyrrolidones [130]. These modifications stabilize and protect them from uptake by the mononuclear phagocytic system (MPS). Targeted therapy has also been demonstrated using liposomes conjugated to monoclonal antibodies via a PEG linker [131], and protease-sensitive polymer-caged liposomes have been developed to enable selective targeting and drug release at the cancerous site by exploiting the natural tendency of affected cells to produce cancer associated proteases to destabilize the liposome [132].

Liposomes also appear to be the preferred carriers for purposes of radionuclide based targeting for cancer therapy. A variety of liposomes such as multi-vesicular liposomes (MUVEL) - small

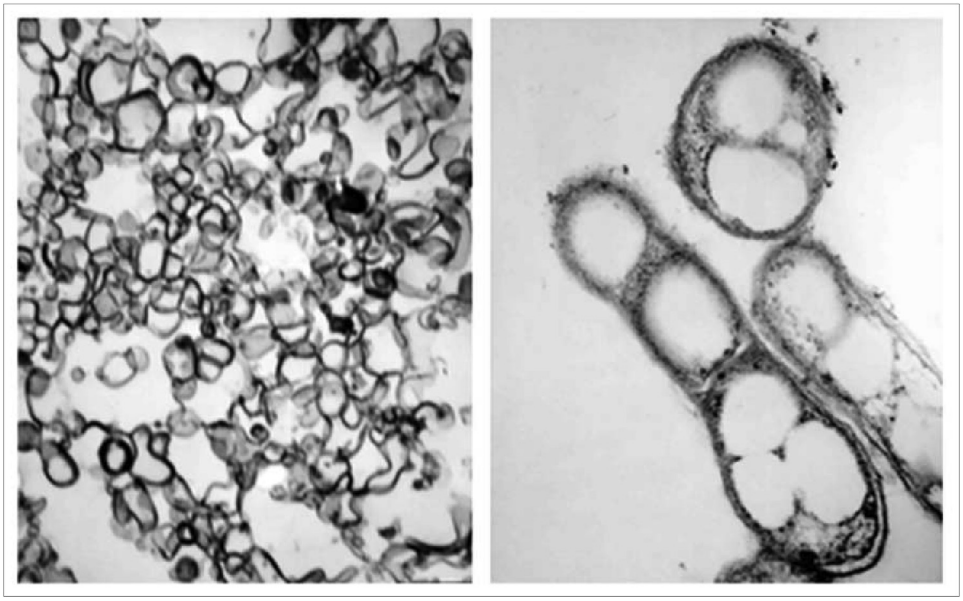

Fig. 6. Electron microscopy pictures of POPC:POPE (6:4) liposomes made using extrusion. Seabra, M.B. (2006) Studies of a Channel-Forming Peptide Inserted into Liposomes formed by POPC:POPS and POPC:POPE, (M.S. Thesis Kansas State University).

vesicles containing radionuclides trapped into large liposomes, polymer coated long circulating liposomes - with low bilayer permeability and low lipid exchange, sterically stabilized liposomes (SSL) - with high load capacity and tumor affinity, etc. have been developed exclusively for this purpose [75,133–135]. The therapeutic efficacy of targeted radiotherapy is due to the tumor's absorption of alpha (α) or beta (β) radiation emitted by the radionuclide. β-emitters such as ^{90}Y, ^{32}P, ^{89}Sr, ^{186}Re, ^{153}Sm, ^{177}Lu, and ^{131}I are by far the most widely utilized radionuclides as therapeutics and alleviation of bone pain [136]. β-electrons have low linear energy transfer (LET) values and long path-lengths. They can pass through tissue, and interact with atoms via energy loss causing ionization, generating free radicals thus causing DNA damage by inducing single strand breaks. On the other hand α-particles have high LET values and shorter path lengths, and are used to generate more localized cellular effects with high chromosomal damage during mitosis and irreparable double strand DNA breaks. Short half-life α-particles emitters such as ^{225}Ac, ^{211}At and ^{213}Bi are commonly employed for targeted alpha particle therapy (TAT) [137,138]. Naturally varying considerations exist in the selection of liposomal carriers based on whether they are employed for beta- or alpha-radiation therapy. For instance studies relating to the effect of surface charge of the liposomes on the radionuclide delivery demonstrated that the use of neutral lipids such as DMPC-Cholesterol in liposomal preparation substantially increased the effective maximum absorbed dosage of beta emitters such as ^{32}P, ^{67}Cu, ^{90}Y and ^{131}I at the tumor site as opposed to cationic DC-cholesterol lipids. On the other hand a study performed on cholesterol stabilized PEGylated liposomes with ^{225}Ac and ^{213}Bi showed high retention of the radionuclide and daughter isotopes only where larger cationic liposomes were involved [139].

Generally speaking, due to the low LET values exhibited by beta electrons, considerations of liposomal rupture due to beta-emissions are not as critical as in the case of alpha emitters where the high LET values of alpha particles coupled with the high energy recoil generated during the formation of daughter nuclides can damage and rupture the liposomal membrane. Moreover, the greater availability of beta-emitters for radiotherapy enables a greater choice in the selection of radionuclides as opposed to those employed in alpha-particle therapy. The ^{225}Ac used in most alpha particle therapies has a chemistry that is not well understood; and that precludes the effective utilization of these emitters in chelate complexes and from integration in larger compounds for the purposes of liposomal encapsulation. Time is yet another factor to be considered in case of radiotherapy. Unlike conventional drugs, radioactive moieties can rapidly decay over time, thus losing therapeutic potency. This is especially true in cases of radionuclides such as ^{213}Bi ($t_{1/2}$ = 45.7 min), where the long times taken for liposomal preparation come at the expense of decreasing therapeutic dosage.

Despite their versatility, biocompatibility, relative non-toxicity and wide application platform, liposome preparation is lengthy and tedious, and preparation steps have to be very carefully monitored to ensure reproducibility in size and entrapment efficiency [128]. Moreover, liposomes have been demonstrated to alter the pharmacokinetic properties of the drugs and are prone to systemic leakage [140]. All of these parameters must be factored in while selecting liposomes as candidates for therapeutic delivery.

2.3.1.1. Polysaccharide vesicles. This class of vesicles is less common. Dextran, chitin, chitosan and their derivatives have been investigated for their use as drug carriers. Most of the vesicles in this category are modified polysaccharides adducted with either small (trimethyl-) [141,142] or larger (3-pentadecylphenol-) [143,144] hydrophobic groups to render them amphipathic. Chitosan derived polymer vesicles are the most studied in this category. Due to their membrane-penetrating ability, these vesicles, palmitoyl glycol chitosan vesicles, are a good choice for intranasal, or oral administration of gut-labile molecules [145,146].

2.3.2. Niosomes

Niosomes or Non-ionic surfactant vesicles (NSVs) are nanoscopic lamellar structures that self-assemble into closed bilayers upon hydrating a preparation of non-ionic surfactants such as alkyl or dialkyl polyglycerol ethers; cholesterol and a charge-inducing agent [147]. They were first reported in the 1970s by researchers

in the cosmetic industry [148,149]. Niosomes were developed and patented by L'Oreal in the 1970s and 1980s and introduced in 1987 by Lancôme [150,151]. Examples of non-ionic surfactants used to generate niosomes include, C_{16} monoalkyl glycerol ether, sorbitan esters, and others.

Niosomes are capable of entrapping hydrophobic and hydrophilic solutes [152]. They can be unilamellar or multilamellar depending on the method of preparation. In many ways Niosomes are liposome analogs and are prepared much like liposomes through non-spontaneous processes involving the input of energy in the form of heat, ultrasound, physical agitation, application of pressure or a combination thereof [153]. Consequently, just like liposomes, most NSV preparation methods involve some hydration of the non-ionic surfactant at an elevated temperature followed by an optional size reduction to obtain the colloidal suspension [154]. Negatively charged molecules such as dicetyl phosphate (DCP) and phosphatidic acid, or positively charged molecules such as cetylpyridinium chloride and stearylamine (SA) can be added (2.5–5 mol%) to prevent aggregation and stabilize the niosomal bilayer [152,153].

There are some fundamental distinctions. While liposomes are made up of neutral or charged double chained phospholipids; niosomes are made up of uncharged single chain surfactants. And since non-ionic surfactants are more stable to enzymatic attack and resistant to air-oxidation than phospholipids, preparing quality niosomes is quite simple [148]. Liposome preparations are expensive owing to their need for special storage and handling due to their predisposition to breakdown when exposed to air.

When water-soluble carrier biomolecules such as sorbitol, sucrose stearate, maltodextrin, etc. are coated with a thin film of dry non-ionic surfactant, the resulting preparation is termed 'proniosomes' [155]. These proniosomes when hydrated generate niosomes. Since proniosomes are obtained as a dry powder; they can be formulated to make beads, capsules or tablets with convenient unit dosing and demonstrate reduced aggregation, fusion, leakage and increased drug entrapment efficiency [150,156].

Niosomes, due to the presence of lipophilic and hydrophilic domains can incorporate drugs with a wide range of solubilities, and indicate potential applications for the delivery of numerous pharmacological agents [150]. Niosome preparations have been investigated for the purposes of drug, gene and vaccine delivery through parenteral, oral, ocular, pulmonary and transdermal routes. The breadth of these studies precludes them from comment in this thesis. Marianecci et al. [154] provides an excellent and comprehensive review on the numerous potential applications of niosomes. Another interesting property of niosomes is their ability to deliver drugs via topical application. Dermal/transdermal drug delivery is a less invasive route for the localized delivery of high concentrations of drugs, by passing the limitations associated with systemic circulation and/or gastrointestinal degradation. The *stratum corneum* of the epidermis works as a barrier for permeation and consequently severely restricts the administration of most drugs through transdermal routes [156]. Niosomes loaded with drugs demonstrate enhanced permeation characteristics and niosomes formulations demonstrated greater skin permeation of enoxacin and higher stability of tretinoin when compared to their respective liposomal counterparts [157,158]. Acid sensitive niosomes generated with Span 60, cholesterol and cholesteryl hemisuccinate (CHEMS) were proposed for the topical delivery of ibuprofen and demonstrated a significant increase in drug penetration through skin [159]. Despite the numerous advantages niosomes have over liposomes, niosomal preparation is generally exhaustive, utilizes numerous moieties, involves the application of non-spontaneous energy consuming processes and takes considerable time.

2.3.3. Polymeric nanocapsules (polymersomes)

Block copolymers are synthetically linked segments of hydrophobic and hydrophilic polymeric units to generate the amphipathic molecule. The segments of block copolymers can be entirely synthetic, semi-synthetic or composed of biopolymers like polypeptides. Like phospholipids, these amphiphiles self-assemble into various ordered structures [58,160,161]. Vesicles formed from block copolymers are commonly referred to as polymersomes and are among the best characterized of the polymeric vesicles. By controlling the formula weight of the blocks, polymersomes with different properties are generated, including ones that vary in-elasticity, permeability and mechanical stability. By their very nature, polymeric building blocks allow for greater chemical diversity than lipids [162]. Due to their higher molecular weights, polymersomes are inherently thicker, tougher and more stable than conventional liposomes. It has been shown that polymersome membranes sustain dilatational strains up to 40–50% when compared with ~5% or less for lipid membranes [163]. A coarse grain molecular dynamics simulation supports the experimental observation that while lipid membranes require only about ~5% strain rate for rupture, while it takes 20% or more to rupture copolymer membranes [164]. Also polymersomes (Fig. 7) can be designed to be responsive to environmental factors such as pH, temperature, redox potential, magnetic field, light and ultrasound [162]. There are a number of comprehensive reviews on this topic [165,166]. Numerous variants of the block polymers have been tested in vitro for their ability to encapsulate and deliver cargo.

2.3.3.1. Peptide containing vesicles. Peptides derivatives linked to synthetic molecules form many different nanostructures: tubes, fibers, rods, micelles, vesicles, doughnuts, bilayers and others [167–173].

Vesicular structures, composed entirely of pure peptides, are relatively rare. Block copolymer monomers composed entirely of polypeptides (i.e. Ac-V_mK_n-NH_2, Ac-G_mD_n-OH, Ac-V_6D-OH, or Ac-KA_6-OH) have been reported to form vesicles [140,174,175]. Upon surveying the published works describing peptides that form vesicles, few were found compared to the many synthetic polymers capable of self-assembling into vesicles. The field of peptide vesicles is still in its infancy but growing at a rapid pace. Vauthey et al. (2002) [172] were the first to show that a simple 7–8 residue amphiphilic peptide is capable of self-assembling into nanotubes and nanovesicles. They called these peptides, "Surfactant-Like Peptide". Santoso et al. (2002) [174], designed similar peptides as the ones by Vauthey et al. (2002) [172] with glycine and aspartic acid capable of self-assembling into nanotubes and nanovesicles.

Peptide amphiphiles capable of self-assembling into nanovesicles can be a simple polypeptide sequence, or a more complex molecule, characterized by the addition of an alkyl chain or with a hydrophobic amino acid segment joined to a hydrophilic sequence (Fig. 8). The associating and stabilizing forces that direct lipid vesicle formation also apply to other polymeric vesicles comprised of long acyl chains attached to peptide amphiphiles. Some examples of designer peptide amphiphiles that form nano structures include G_nD_2, A_6D, V_6D, V_6D_2, A_6K, I_3K, A_6K_2, GAVILRR, $A_2V_2L_3WE_{(2\text{ or }7)}$ and similar peptides. In addition, amphiphilic block macrocyclic-copolypeptides have been used to generate bioactive nanovesicles that incorporate the arginine rich human immunodeficiency virus type-1 Rev protein to target the assembled vesicles. The macrocyclic protein sequence also includes tryptophan residues that add stability potentially through Pi-Pi stacking interactions [176]. The Sherman group employed a host-guest approach to drive self assembly using the macrocycle Cucurbit[8]

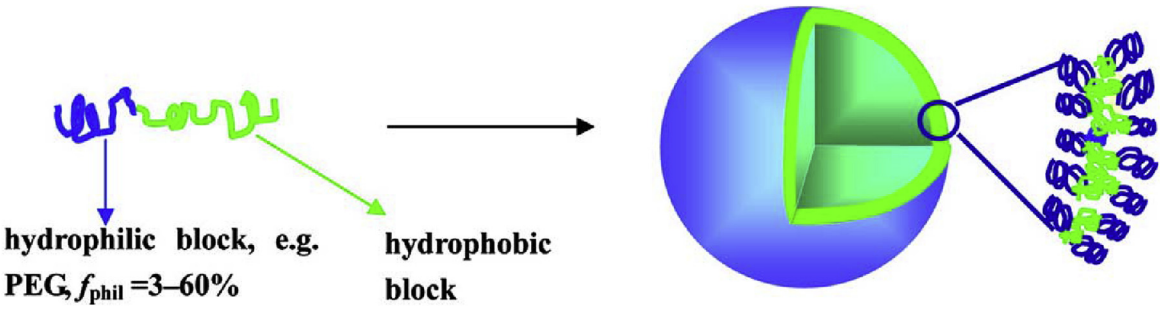

Fig. 7. Polymersomes derived from asymmetric block copolymers. Reprinted (adapted) with permission from Meng et al. (2009) *Biomacromolecules*, **10**(2), 197–209. Copyright 2009 American Chemical Society [156].

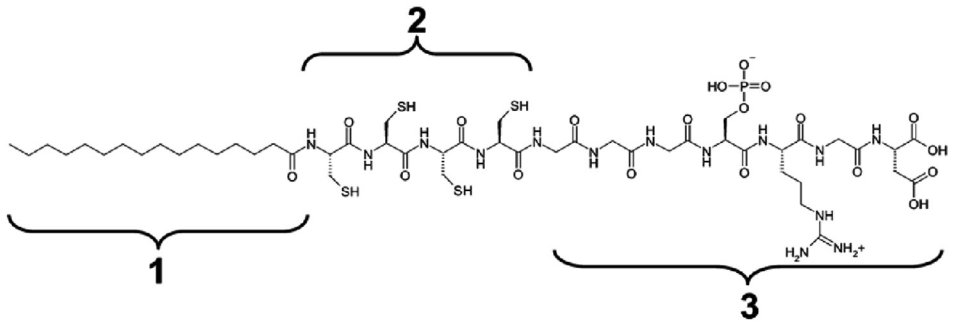

Fig. 8. Peptide amphiphile structure. The basic structural components of peptide nanoparticle components: (1) a hydrophobic tail, (2) lower, rigid part, including 4 cysteine residues (3) upper, flexible part, including 3 glycines, a phosphoserine group and an integrin-binding motif, RGD. "Reprinted (adapted) with permission from Tsonchev et al. (2004) [173].

uril (CB[8]). The ternary host complex formed by CB[8] bound two guest pyrene ligands yielding a tight binding constant with a CAC of 12 μM. This assembly generated larger vesicles ~150–250 nm in diameter [177]. Subsequently the same group was able to load the vesicles with basic fibroblast growth factor, retain it and subsequently release it for uptake by fibroblasts [178]. A third group was able to prepare bilayer-delimited vesicles in the 60 nm size range using a simple peptide Ac-Ala-Ala-Val-Val-Leu-Leu-Leu-Trp-Glu_2-COOH under acidic conditions [179]. The SA2 peptide has a CAC of around 50 μM and was able to entrap calcein [180]. These vesicles not only carry the advantage of being more biocompatible and biodegradable than other synthetic and semi-synthetic polymer vesicles and they where shown to be more stable than lipid and polysaccharide vesicles [179]. Recently another group studied the same SA2 assemblies using biophysical and computational tools to produce a visual model of the vesicles [181].

Reviews by Zhao et al. (2010) [175] and Zhang, S (2002) [182] summarize the various peptide amphiphiles that form nano structures and discuss a more exhaustive list of the various peptide amphiphiles. Some studies reported the use of oligo valines to promote inter-digitation, the mixing of oppositely charged peptides to reduce the critical aggregation concentration (CACs), and hydrophobic sequences containing complimenting small and large amino acids [183]. The hydrophobic chain length plays a critical role in the final assembly. Typically, the size of the hydrophobic tail in such peptide amphiphiles is about 3–9 hydrophobic residues. The length of the hydrophobic tail can determine the thickness of the outer layer of such nano structures but with longer chain lengths comes the issue of solubility and conversely, shorter chain lengths decrease the propensity of aggregation. Hence a balance of chain length is required for the desired property. This is achieved by increasing or decreasing the length of the hydrophilic segments of the molecule.

2.3.3.1.1. Branched amphiphilic peptide capsules (BAPCs). These structures represent a novel class of nanocarriers. First described by Gudlur et al. [184] in 2012, they are self-assembling structures where a water filled cavity is surrounded by an amphiphilic branched peptide bilayer. They are stable, biocompatible nanocarriers that are structurally similar to liposomes and polymersomes. The properties, applications and biophysical characterization of these carrier systems will be discussed at length in section 4.

3. Peptide vesicles stabilized by beta-sheet secondary structures

Most self-assembling peptide based polymeric vesicles either lack a defined secondary structure or adopt helical conformations in their assembled structures. Recently, however, vesicular [185–187] and micellar [160,188,189] assemblies stabilized by β-sheets have been reported. Gebhardt et al. studying poly(-butadiene) -poly(L-lysine) co-block polymers elucidated the effects of secondary structure on the morphology of vesicles [187]. In the case of poly(butadiene)$_{107}$-poly(L-lysine)$_{27}$ coblock polymers, the transition from α-helix to β-sheet takes place at a pH above the pKa (>10.5) of the lysine side chains. This transition resulted in a slight increase in the hydrodynamic radii of the vesicles and the overall assembly remained intact as determined by dynamic light scattering (DLS) and static light scattering (SLS). The formation of parallel β-sheets between the corona chains at the vesicular interface served to release interfacial curvature by creating a flatter interface. A molecular dynamics simulation study on the self-assembly of peptide amphiphiles [190] showed an interplay between hydrophobic interaction between the alkyl chains and hydrogen bonding between the peptide blocks, resulting in assemblies that were spherical β-sheets, micelles with β-sheets in the corona, and long cylindrical fibers (Fig. 9).

4. Studies on branched amphiphilic peptide capsules

4.1. Origin of the BAPC sequences

The concept of building diacyl phospholipid orthologs made up of just amino acids is not particularly new, however identifying a functional self-assembling sequence(s) is. The sequences used for the self-assembling branched amphipathic peptide vesicles evolved from earlier studies on several adhesive peptides. Previously, several peptide constructs were identified that produced nanofibrils with mechanical adhesive properties due to entanglement [191,192]. The hydrophobic core sequence used in the adhesives occurs in nature as an internal fragment of the human dihydropyridine sensitive L-type calcium channel segment, CaIVS3 (DPWNVFDFLIVIGSIIDVILSE). The underlined segment is a portion of one of the transmembrane helices that contribute to the central water-filled pore of this channel [193,194]. Lyophilization of the synthesized CaIVS3 peptide resulted in insoluble clumps resistant to mechanical disruption suggested that strong cohesive forces were driving this association. An α to β transition for the 9-residue sequence was observed that could be controlled predictably by adding charged amino acid segments to both ends of the underlined sequence (h_9) (Table 1) and by varying the pH [191,192]. An assay was used that measured the strength (MPa) required to shear (pulled at 180°) two glued cherry wood strips treated with a 4% w/v solution of the peptide dissolved in water and then adjusted to the indicated pH values before hot pressing the samples (Fig. 10). The sequences with the flanking tri-lysine or tri-diaminopropionic acid (DAP) segments performed best at pH 12.0, conditions in which the amino groups of the Lys and DAP residues are mostly deprotonated thereby increasing the hydrophobicity of the peptides. The DAP amino acid is a shortened lysine analog with just one methyl group on its side chain as compare to the four methyl groups in lysine. There were no statistical differences between the two different cationic residues or increasing the number of h_9 hydrophobic segments.

Table 2 summarizes the shear strength and hydrophobicity for a number of FLIVIGSII derived sequences. The two longer sequences simply incorporated the naturally occurring C- or N-terminal hydrophobic residues present in the CaIVS3 sequence. The shorter sequences represent truncated versions of the h_9 sequence and in some cases include single amino acid substitutions. Several known amyloid peptides as well as a twitter-ionic sequence were tested as controls.

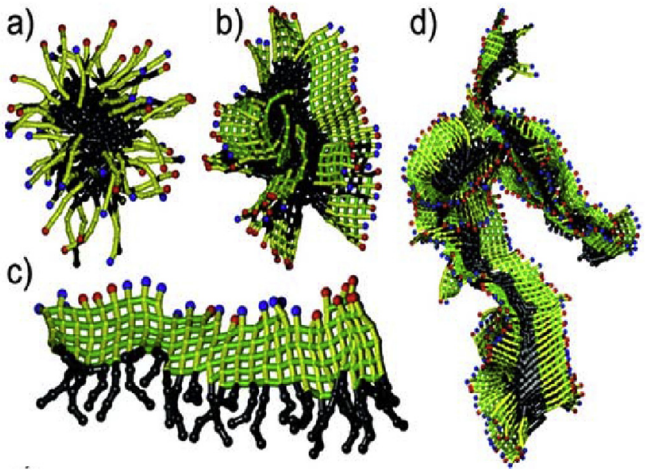

Fig. 9. Snapshots from molecular simulations of peptide amphiphiles. "(a) The spherical micelle, (b) the micelle with β-sheets on the outside forming the corona, (c) the β-sheets, and (d) the fiber aggregate". [Reprinted (adapted) with permission from Velichko et al. (2008) [190], *J. Phys Chem B.*, 112(8), 2326–34. Copyright 2008 American Chemical Society.].

Table 1
Adhesive peptide sequences [191]. Abbreviations: X = diaminopropionic acid.

Peptide	Sequence	MW (Daltons)
Eh_9E	EEEFLIVIGSIIEEE	1748.9
Kh_9E	KKKFLIVIGSIIEEE	1746.1
Eh_9K	EEEFLIVIGSIIKKK	1746.1
Kh_9K	KKKFLIVIGSIIKKK	1743.3
$(Kh_9)_2K$	KKKFLIVIGSIIKKKFLIVIGSIIKKK	3084.1
$(Kh_9)_3K$	KKKFLIVIGSIIKKKFLIVIGSIIKKKFLIVIGSIIKKK	4428.8
Xh_9X	XXXVLIVIGSIIXXX	1490.8

There are three h_5 sequences (*alpha*, *mezzo* and *omega*) derived by frame shifting a five-residue window within the h_9 sequence. In addition, four unrelated β-forming sequences were tested. The first three $A\beta_{16\text{-}21}$, $A\beta_{30\text{-}35}$, and $IAPP_{22\text{-}28}$ were reported nucleation sites for amyloid fiber formation and have sequences that closely resemble that of $K_3h_{5\alpha}K_3$. The last sequence, KAE_{16}-IV, contains both basic and acidic residues and should not display any pH dependence.

With the exception of KAE_{16}-IV, all of the sequences showed adhesive properties when dry pressed at 130 °C. The shorter $h_{5\alpha}$ containing sequence required the most force to shear the union holding the strips together. It was determined that this shorter sequence had the lowest free energy for the packed assembly and was the most hydrophobic. While reducing the size of the hydrophobic core sequence increased strength, reducing the number of flanking lysines from three to two had a negative effect on adhesive strength. All of the CaIVS3 derived sequences acted as adhesives even when the dry press temperature was reduced, although with decreased strength. However the amyloid derived sequences displayed no adhesive properties if heating was omitted during pressing. Several of the sequences showing strengths above 3 MPa were tested for their wet strength after emersion for 48 h (Table 3).

Structural analyses were conducted on both soluble peptides (CD) and dry pressed peptide (FTIR) processed at pH 12.0. All of the dry pressed peptides showed β-structure. Only $K_3h_{5\alpha}K_3$ and $K_3h_9K_3$ showed β-structure in water. $K_3h_{5\Omega}K_3$ and $K_3h_{5M}K_3$ showed β-structure only in ethylene glycol. No structure was observed for the amyloid forming peptides with either solvent.

In parallel, transmission electron microscopy was used to visualize the assemblies being generated at pH values of 12.0, 2.0 and 7.0 (Fig 11). The images taken at pH 12.0 show entangled nanofibers. Regarding the adhesive properties the peptides, they only bonded with rough surfaces. When the peptides were used to glue smooth glass slides together shear strengths of just ~1.5 MPa were required to separate the two pieces. If the slides were siliconized the peptides showed no effect in joining the glass slides.

Table 4 compares the different properties of the nano-fiber forming sequences. It is clear that the hydrophobic core sequences of FLIVIGSII and FLIVI have unique structural properties, in particular their ability to associate and assemble as a β-structure in water and their wet adhesive strength. Even though the $K_3FLIVIK_3$ sequence appeared unstructured in water at pH 2.0 and 7.0, transmission electron microscopy images were taken these sequences that were applied as solutions to the TEM grids and allowed to dry (Fig. 11).

The images show two distinct structures–at pH 7.0 the peptides associate to form a soot-like fractal while at pH 2.0 they resemble lipid micelles. Upon viewing the pH 2.0 structures and recalling that linear lipid detergents or soap amphipaths make similar micellar structures and that branched lipid amphipaths such as

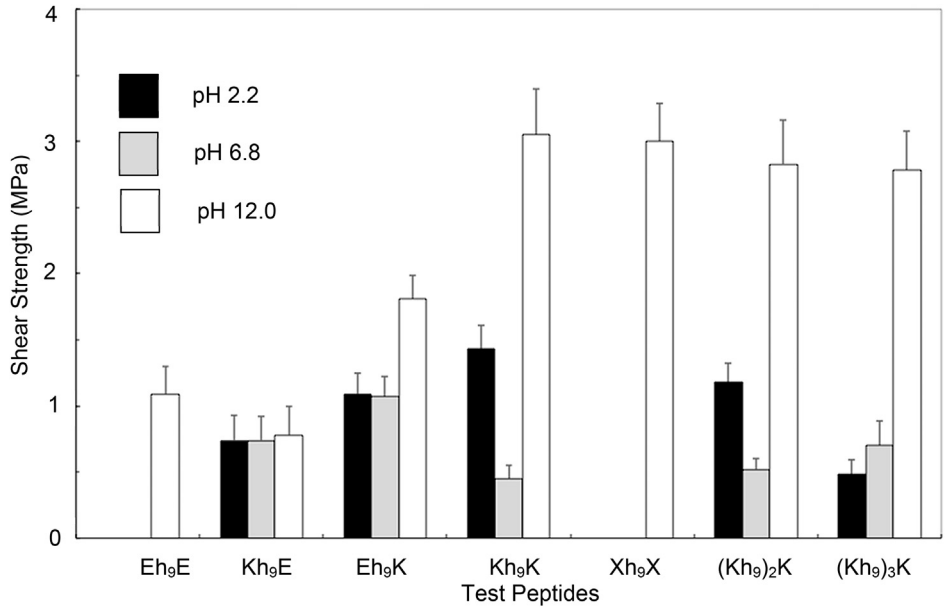

Fig. 10. Shear strength of peptide adhesives measured in Mega Pascals (MPa) with different tri-residue segments flanking the h_9 sequence. E, K and X represent the tripeptides $(Glu)_3$, $(Lys)_3$ and $(diaminopropionic\ acid)_3$, respectively. Peptide solutions– 4% (360 μL) were spread onto marked 8.0 cm by 2.0 cm areas on one side of two separate strips of wood. The coated strips sat for 15 min at RT, before being pressed together for 5 min at 130 °C and 1.4 MPa cm^{-1}.using a Hot Press Model 3890 Auto M (Carver Inc., Wabash, IN). The glued strips were then conditioned for 3 days at 50% relative humidity and 23 °C before being cut into test sized pieces. Reproduced from Shen et al. [191].

Table 2
Correlation of shear strength and hydrophobicity for a number of peptides showing adhesive properties [192]. Samples were prepared as described in Fig. 10.

Peptides	Sequences	Shear strength (MPa)	G_{avg} (kcal/mol)
$K_3h_9K_3$	KKKFLIVIGSIIKKK	3.0 ± 0.1	−0.46
$K_3h_{11}K_3$	KKKVFFLIVIGSIIKKK	2.9 ± 0.2	−0.48
$K_3h_{12}K_3$	KKKFLIVIGSIIVILKKK	2.2 ± 0.1	−0.50
$K_3h_7K_3$	KKKFLIVIGSKKK	2.6 ± 0.2	−0.42
$K_3h_{5\alpha}K_3$	KKKFLIVIKKK	3.3 ± 0.2	−0.62
$K_3h_{5M}K_3$	KKKIVIGSKKK	3.4 ± 0.2	−0.37
$K_3h_{5\Omega}K_3$	KKKIGSIIKKK	3.2 ± 0.2	−0.31
$K_2h_{5\alpha}K_2$	KKFLIVIKK	2.8 ± 0.1	−0.53
$K_2h_{5\Omega}K_2$	KKIGSIIKK	2.4 ± 0.2	−0.31
$K_3h_{5ML}K_2$	KKKIVLGSKKK	3.4 ± 0.2	−0.36
$K_3h_{5MA}K_2$	KKKIVAGSKKK	2.7 ± 0.1	−0.35
$A\beta_{16\text{-}21}$	KKKLVFFAKKK	3.4 ± 0.3	−0.50
$A\beta_{30\text{-}35}$	KKKAIIGLMKKK	3.4 ± 0.1	−0.39
$IAPP_{22\text{-}28}$	KKKIGGAILKKK	2.9 ± 0.4	−0.30
KAE_{16}-IV	$(KA)_4(EA)_4$-$CONH_2$	1.4 ± 0.1	+0.62

Table 3
Comparison between dry and wet strength for select peptide adhesives [176].All samples were used at 4% w/v and hot-pressed at 130 °C. Glue samples were soaked in water for 48 h before wet strength test. Adapted from Mo et al., 2008 [192].

Peptide sequence	Dry strength (MPa)	Wet strength (MPa)
$K_3h_{5\alpha}K_3$	3.3 ± 0.2	1.13 ± 0.3
$K_3h_{5\Omega}K_3$	3.2 ± 0.2	0.66 ± 0.2
$K_3h_{5M}K_3$	3.4 ± 0.2	0.0
$K_3h_9K_3$	3.0 ± 0.2	0.67 ± 0.1

diacylglycerol-phospholipids assemble into liposomes, the idea of altering the sequence from a linear to a branched one with all of the charges or one side was born.

4.2. Shared properties between BAPCS and lipid vesicles

To generate an all peptide bilayer delimited vesicle, the original design included 5 lysines at the C-terminus with the N-terminal lysine used to generate the branch point. The two hydrophobic segments were added simultaneously using standard Fmoc chemistries. It was decided from the beginning to include a mixture of two different sized peptides such that the shorter sequence would compensate for any strain due to curvature. These vesicles were formed from the two 15- and 23-residue branched amphiphilic peptides: bis(FLIVI)-K-K_4 and bis(FLIVIGSII)-K-K_4 commonly referred to as bis(h_5)-K-K_4 and bis(h_9)-K-K_4, respectively (Fig. 12). In 2012, Gudlur et al., first described the formation of these structures at 25 °C (RT) (Fig. 13) [184].

The linear (h_9)-K-K_4 sequence (Fig. 12) did not form any detectable structures. Henceforth these structures will be referred to as branched amphiphilic peptide capsules (BAPCs) to avoid confusion with lipid vesicles.

In Fig. 13, 50–150 nm spherical structures are present after a 2 h incubation period. The BAPCs in this image appear to be fusing. The resolution of these images was insufficient to identify whether or not the capsules were surrounded by a bilayer. Subsequently methyl mercury was added to the bis(FLIVI)-K-K_4 and bis(-FLIVIGSII)-K-K_4 peptides in which the thiol containing amino acid cysteine was added to the C-terminal lysine of both peptide sequences [195]. In this representative image (Fig. 14) of capsules formed at 25 °C, the bilayers are distinct due to the emission of a specific energy x-ray associated with mercury bombarded by electrons. The BAPCs remain water filled and a number of capsules appear to be fusing. Note that unlike many liposome preparations all of the BAPC structures are unilamellar.

Based on computer simulations these peptides behave much like phospholipids. As observed with membrane lipids, the hydrophobic regions of these peptide molecules are poorly soluble in water and in an analogous manner shield themselves by associating to form bilayers in aqueous solutions that appear to be 4 nm in thickness (Fig. 15). The aromatic side chains of phenylalanine residues and other aliphatic residues are buried in the interior of the newly formed membrane.

In addition to the aromatic and non-polar residues interacting

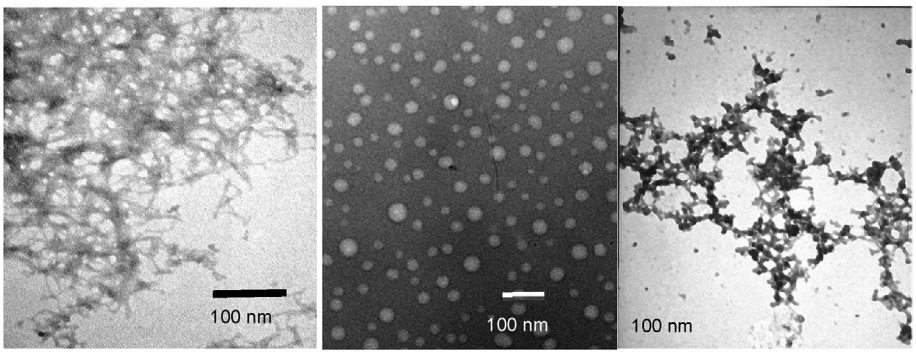

Fig. 11. TEM images of $K_3FLIVIK_3$ that were dried from peptide solutions prepared at different pH values. The left panel is peptide suspended at pH 12.0 and imaged at 70,000× magnification. The center panel is peptide incubated at pH 2.0 and imaged at 34,000×. The right panel is peptide dissolved at pH 7.0 and imaged at 70,000×.

Table 4
Comparison of structural and adhesive properties of test sequences. All sequences were tested in parallel for adhesive strength under different dry press conditions. Assembly properties were measured by analytic ultracentrifugation.

FLIVIGSII, FLIVI	IVIGS, IGSII	IFGAIL, KLVFF, AIIGL
Random structure at pH 2 and 7	Random structure at pH 2 and 7	Random structure at pH 2 and 7
β-structure at pH 12 in water	β-structure at pH 12 in ethylene glycol	No structure at pH 12 in any solvent
β-structure when dried from water	β-structure when dried from water	β-structure only when dry pressed
Assembles in water pH > 9	No assembly at pH 12	No assembly at pH 12
Adhesive after dry press, RT	Adhesive after dry press, 130 °C	Adhesive after dry press, 130 °c
Measurable wet adhesive strength	No wet adhesive strength	No wet adhesive strength
Forms entangled nano-fibrils	Forms entangled nano-fibrils	Forms entangled proto-fibrils

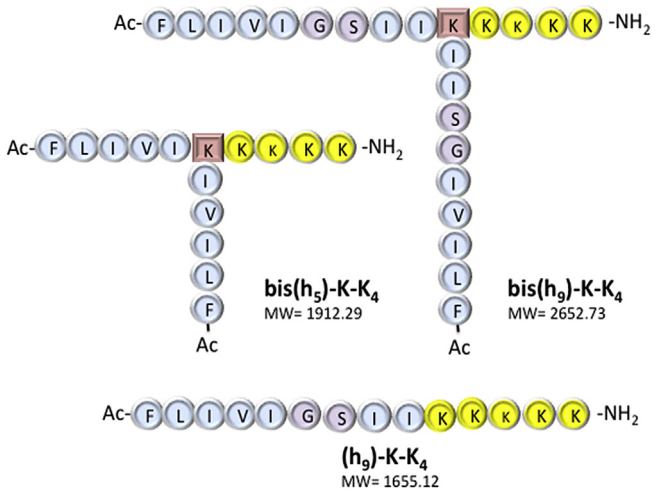

Fig. 12. Graphic representation of the branched and linear amphipathic sequences initially tested. The color coding is added to signify those residues that are cationic (yellow), non-polar (blue) and hydrophilic (violet) along with the branch point (pink).

with each other through hydrophobic interactions; CD and FT-IR indicated significant parallel β-like structure, indicative of hydrogen bonding networks. The positively charged lysines reside in the two aqueous phases, on both the inner and outer sides of the bilayer (Fig. 15). Additionally, this model seems to show a networks of hydrogen bonds between adjacent β-structures that help the organized structure stabilize at very low sub-micromolar concentrations - as judged by dilution studies determined by both CD and ITC—conditions where nearly all phospholipid assemblies would be fully dissociated. We have yet to determine the critical assembly concentrations (CAC) of BAPCs.

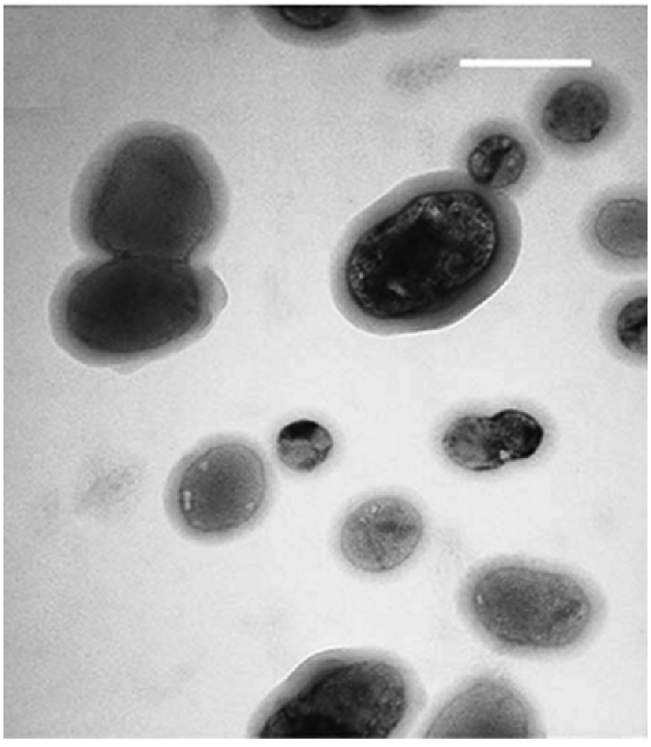

Fig. 13. Transmission electron microscopy (TEM) obtained from the synthesis of nanocapsules solution (1.5 mM). The image shows the process of fusing the nanocapsules, resulting in larger and more elongated structures (scale bar: 200 nm). Reproduced from Gudlur et al. (2012) [184].

4.2.1. BAPC assembly

Nanocapsules formation follows nearly the same steps used for the preparation of diacylglycerol phospholipid vesicles (Fig. 16).

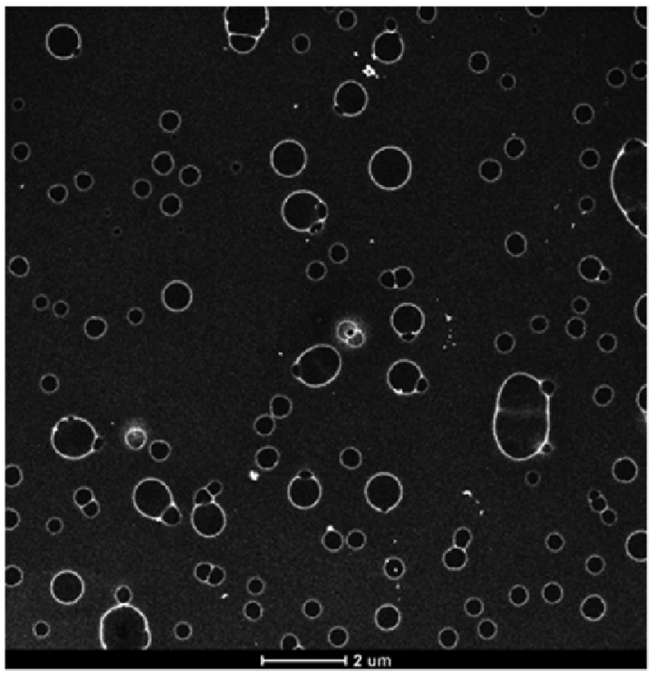

Fig. 14. Scanning transmission electron microscopy (STEM) of Cys containing peptides labeled with Me–Hg 24 h after mixing. Capsules were prepared with the peptides at 0.1 mM with 30% of them containing the Me–Hg. The images were captured using the inverted dark-field mode. Reproduced from Sukthankar et al. [195].

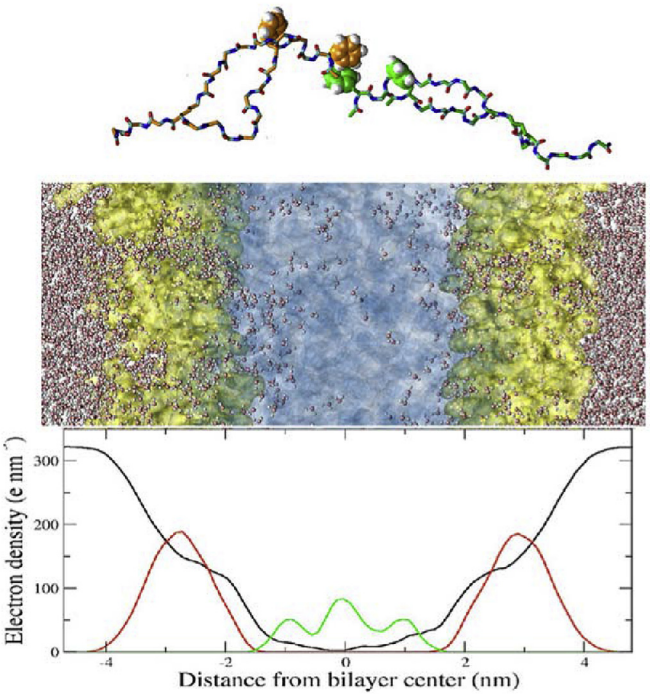

Fig. 15. Atomistic model of the BAPC peptide bilayer. In the center, the peptides are shown in a transparent surface, with Lys colored in yellow and other residues in blue and water in ball-and-stick mode. The top panel illustrates extensive π-π stacking interactions among Phe residues. The bottom panel shows the average electron density profiles of water (black line), Lys (red) and Phe residues (green line) calculated from last 40 ns of the 100 ns simulation.

Initially the two peptides, bis(FLIVI)-K-K_4 and bis(FLIVIGSII)-K-K_4, are dissolved individually in neat 2,2,2-trifluoroethanol (TFE). In this solvent the peptides adopt a helical structure. As helices they are monomeric, thereby ensuring complete mixing of the two sequences when combined. This solvent also ensures that they remain helical upon drying, based on FT-IR studies.

The individual dissolved peptide concentrations are determined using the molar absorptivity (ε) of phenylalanyl residues in the sequence (195 M^{-1} cm^{-1} at 257.5 nm) [184]. The two peptides are then mixed in equimolar ratios to generate desired concentrations and then dried in vacuo. All of the initial experiments limited the ratio to 1:1 to ensure an adequate concentration of the shorter peptide to accommodate the curvature of assembled capsules.

Distilled deionized water or aqueous solution containing solutes for encapsulation are added drop-wise to the dried peptides at the desired temperature. Different secondary structures and capsule sizes are seen when assembly occurs at different temperatures. This will be discussed later.

4.2.2. *Fusion and sizing*

Sukthankar et al. [195] followed the assembly process over 2 h (Fig. 17) and showed that within 5 min of hydrating the mercury-labeled peptides, nano-fibrils appeared which gradually began to group together forming the nanocapsules with a 20 nm average size by 30 min. At 60 min the small BAPCs appeared to coalese and by 2 h have fused into larger capsules. By 48 h, micron sized capsules are present. [184] While these STEM images provide a static view into the underlying assembly events, a solution study was designed to demonstrate the dynamic nature of fusion process (Fig. 18A & B) [195].

The dilution of the self-quenching fluorescent dye Eosin Y was recorded during fusion the process. Two populations of BAPCs, harvested and washed 30 min post hydration, containing either 2.2 mM dye (5 parts) or just water (95 parts), were mixed. At the earliest time points the dye containing BAPCs would be expected to fuse with the water filled ones thereby diluting the dye. This dilution was recorded as an increase in fluorescence. With each 5 min scan the intensity of the dye increased without any dye appearing in the 30 kDa cut-off filtrates, thus demonstrating fusion and the fact that the BAPCs are water filled. Lowering the BAPCs

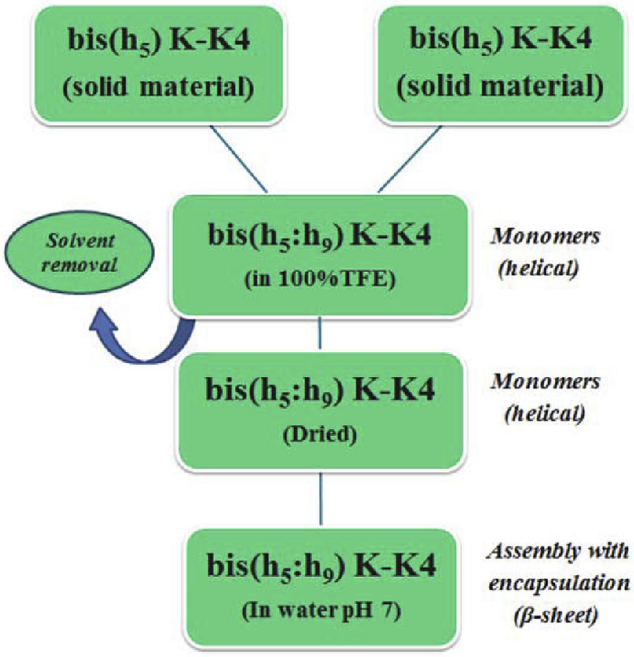

Fig. 16. Assembly protocol for peptides nanocapsules.

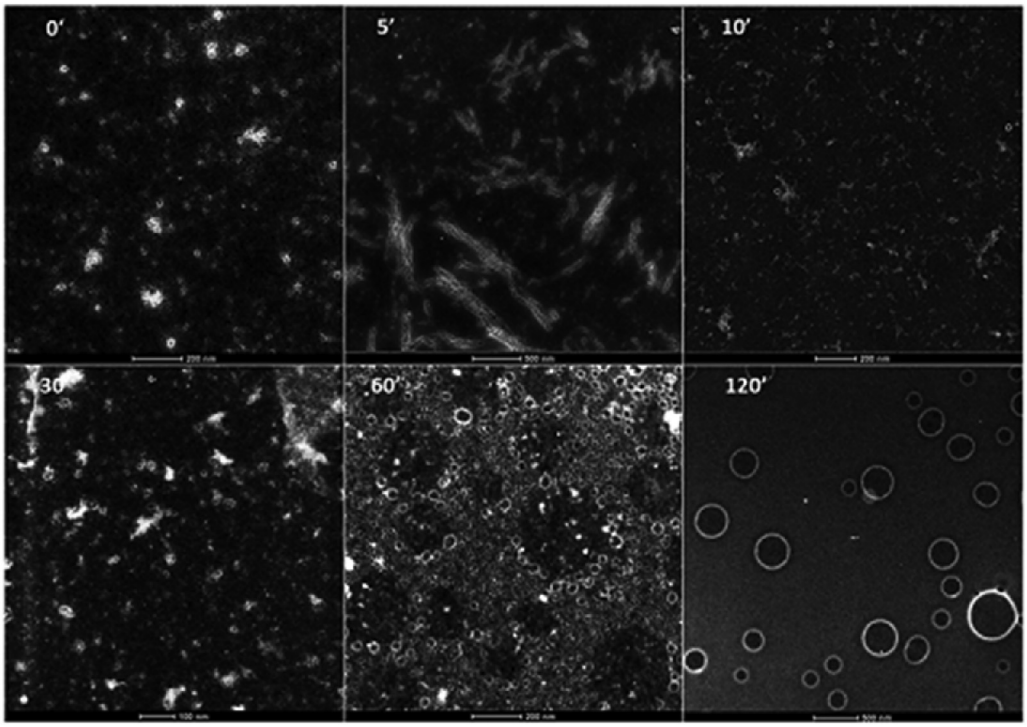

Fig. 17. BAPC fusion time course. Peptides(0.1 mM) bis(FLIVI)-K-K_4 and bis(FLIVIGSII)-K-K_4 containing 30% bis(FLIVI)-K-K_4-Cys-Hg-Me and bis(FLIVIGSII)-K-K_4-Cys-Hg-Me were hydrated with samples removed at the indicated times and dried. The STEM images are displayed in inverted dark field. The scale bar at the bottom of the micrographs are 200 nm, 500 nm, 200 nm, 100 nm, 200 nm and 500 nm, for the intervals of 0, 5, 10, 30, 60, and 120 min, respectively. Reproduced from Sukthankar et al. [195].

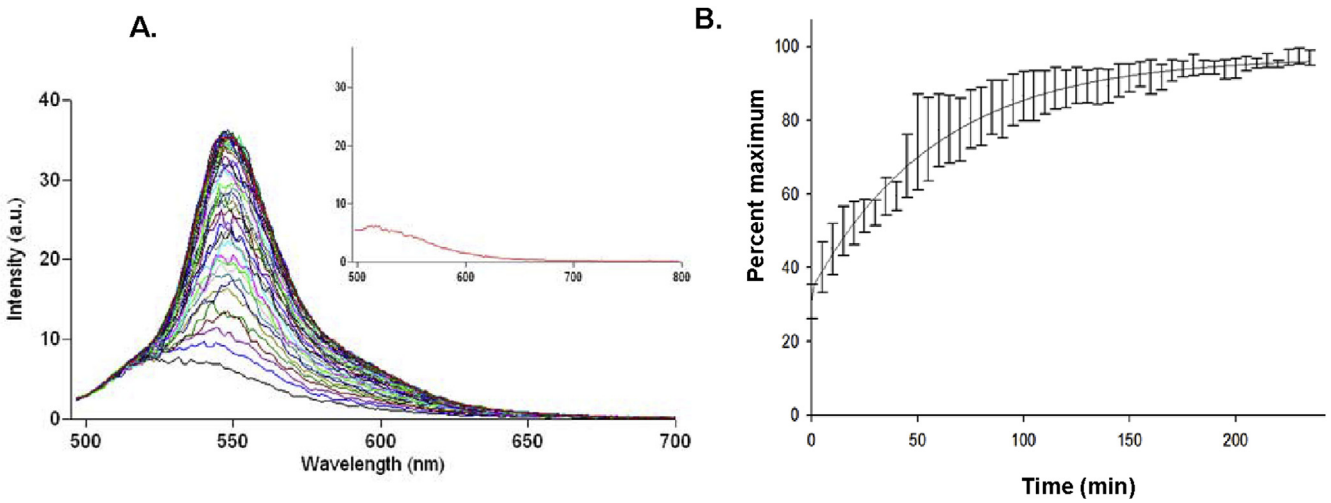

Fig. 18. BAPC Fusion Study. Panel A. Salt washed eosin Y trapped BAPCs were mixed with water filled BAPCs at 25 °C. Fluorescence scans were taken at 5 min intervals for 235 min. The inset shows spectrum of sample stored at 4 °C for 6.5 h. The units shown are identical to those in A. Panel B. Measured maximum eosin fluorescence intensity as a function of time during the fusion reaction. The t = 0 represents quenched value of salt washed eosin encapsulate in the capsules (2.2 mM). The data was fitted to a second order exponential with the error bars representing the SEM with n = 3. Reproduced from Sukthankar et al. [195].

temperature to 4 °C at t = 35 min (inset to Fig. 18A) shows that the fusion process can be stopped. Returning the 4 °C sample to RT did not restore fusion. This phenomenon is addressed later in Section 4.3.2.

Since the BAPCs fuse like liposomes, resizing of larger BAPCs was tested using polycarbonate filters using methods commonly employed to prepare small phospholipid vesicles (SUVs). Starting with a 24 h, 25 °C sample (200–500 nm diameter BAPCs) the BAPCs were extruded through a 100 nm pore filter, yielding a mixed population, 20–60 nm diameter capsules. Few if any 100 nm capsules were seen suggesting this size is disfavored over smaller ones. Those BAPCs were then extruded a second time through a 30 nm filter resulting in a relatively homogeneous population with sizes ranging from 20 to 30 nm. The 30 nm membrane is the smallest commercially available and attempting to go even smaller does not appear feasible since the BAPCs assemble as 20–30 nm structures. Once resized to 20–30 nm, the BAPCs should be cooled to 4 °C at RT to prevent their re fusion.

The inset to Fig. 18A showed that lowing the temperature to 4 °C after incubating at 25 °C for 35 min resulted in an altered BAPC that

was no longer able to fuse. Even increasing the temperature stepwise to 80 °C failed to restart fusion. In addition, the cooled BAPCs were no longer susceptible to disassembly in 50% TFE/water containing solutions. Based on these results the effect of temperature on BAPC properties were initiated. The results from these experiments indicate that there is a temperature dependence for assembly.

4.3. Distinctive properties of BAPCs

4.3.1. Temperature effects on BAPC formation

BAPC assembly was monitored at multiple temperatures with their final secondary structures determined [196]. To briefly summarize, BAPCs formed at 4 °C and 37 °C yield uniform BAPCs that are 20–30 nm in diameter, do not fuse yet are disassembled in 50% TFE. The 4 °C BAPCs are predominantly unstructured while the 37 °C display beta-like structure. The BAPCs formed at 25 °C were the only ones that displayed the fusogenic property and disassembled in 50% TFE. They displayed secondary structure that appear to be a mixture of random coil and beta-like structure. Over time as the BAPCs grew in size they became more beta-like in structure. It was hypothesized that the mixture of random and beta structure is higher energy and meta-stable and that fusion leads to a lower free energy state. Assembly at 25 °C for 30 min followed by 1 h of cooling at 4 °C and then rewarming to temperatures >25 °C makes the BAPCs even more stable and resistant to disassembly in 50% TFE. Their structures changed during the experiment from a combination of random and beta at 25 °C to mostly random at 4 °C and then back to mixed upon rewarming. It was postulated that during the thermal cycling entanglement of the hydrophobic segments occurred during the transition from random coil back to the mixed conformer. This unusual BAPC is referred to as being in a “locked” conformation. This particular BAPC has proven to be useful in delivering DNA to cells (not discussed in this review).

4.3.2. BAPC stability

The thermal stability of the nanocapsules was also evaluated by Gudlur et al. [184], using Differential Scanning Calorimetry (DSC) for temperatures ranging from 20 to 95 °C. This experiment was confirmed over the same temperature range using BAPCs containing the quenched dye Eosin Y (2.1 mM). No fluorescence intensity increase was observed over the full temperature range indicating that the BAPCs did not rupture and release contents. The lack of a phase transition over this temperature range indicates maintenance of the bilayer's structural and functional integrity. This observation is important because phospholipid membranes comprised of acyl chains of 18 carbons or less with no double bonds generally exhibit phase transition temperatures between 35 and 55 °C [197]. At these temperatures, lipid vesicles tend to become permeable. This propertyis a disadvantage due to the release of internal contents when exposed to elevated temperatures. In addition to thermal stability the BAPCs are resistant to proteases, chaotropes, dodecylsulfate and dilution [184].

4.3.3. Cellular uptake

As showed by Sukthankar et al. [198] nanocapsules are formed with an average diameter of 20–30 nm with an internal volume of 4000 nm^3 allowing them to be considered as possible candidates for the encapsulation of a large number of different molecules including proteins. For this purpose BAPCs were used to encapsulate TAMRA-labeled TRNase A (RNase A, 13.7 kDa) and TAMRA-labeled cytochrome c (Tcytc, ~12 kDa). These apoptogenic proteins were chosen since their release from the BAPCs would trigger a measurable cytotoxic effect. For the positive delivery control the amphipathic peptide called Pep-1 was employed. This peptide reagent is known to induce cellular uptake of proteins and peptides [199,200].

Both cytochrome c and RNase A were successfully encapsulated in the BAPCs and efficiently delivered into HeLa cells (Fig. 19). In the images obtained we observed a slightly lower signal when comparing the transport of Tcytc using BAPCs with the control Pep-1.

Both cytochrome c and RNase A are known for their apoptotic effects [201,202]. This BAPC experiments do not record any obvious signs of apoptosis whereas the transport mediated by Pep-1 exhibited the expected effect of cellular cytotoxicity. This was the first experiment that indicated that the cell's degradative machinery did not act on the BAPCs. This study (Fig. 20) also showed that the BAPCs are retained intact in HeLa cells for long periods of time. The images generated with confocal microscopy revealed that even after 14 days, the BAPCs labeled with Rhodamine B persisted inside the HeLa cells and interestingly are transferred without any apparent degradation to the daughter cells formed during mitotic divisions.

4.3.4. In vivo studies-encapsulated alpha-emitting radionuclides

The remarkable stability of BAPCs makes them singularly useful in several applications and ill suited for others. Given their temperature stability and flexibility (based on resizing results) BAPCs were used to encapsulate an alpha-particle emitting radioisotope. Molecular nuclear medicine plays important roles in the diagnosis and treatment of cancer. Depending on the radioisotope's properties, the compounds can be used for diagnostic and/or therapeutic purposes. Targeted alpha-particles have a significant advantage in targeted radiotherapy because of their high potency, specificity as well as their ability to kill non-proliferating cells and without the need for oxygenation [203]. Current targeted alpha radioimmunotherapy takes advantage of the specificity of antibody-conjugated radionuclides to deliver biocidal radiation to cancer cells [204]. Alpha-emitting radionuclides such as Actinium-225 and Bismuth-213 are commonly used for this purpose. This method does have some disadvantages in that the high energy of the ejected alpha particle can collide with and destroy the covalent bond between the chelator molecule and the antibody. Also the energy released during the recoil of the daughter nuclide is sufficient to dislodge the radionuclide from the chelator itself. This release of free radionuclides can cause off-target accumulation and potential damage [205].

For the BAPC encapsulation studies ^{225}Actinium was tried. This radionuclide has a T½ = 9.92 days while releasing 4 α-particles as it decays to ^{209}Bismuth [203]. Alpha particles are emitted with a velocity of 5% the speed of light. The average energy of the 4 ejected helium nuclei is 6.93 MeV [203]. The average mass of the daughter nuclei must have equal and opposite momenta which accounting for the mass difference calculates to an average energy of 0.13 MeV. As shown in Fig. 21 the BAPCs are able to retain 95% of the radionuclides (parent and daughters) for 7 days. As previously mentioned theoretical calculations by Sofou et al. [134,135] suggest negligible (<0.001%) daughter retention for the last isotope of ^{225}AC for 100 nm diameter liposomes and 50% retention for liposomes with a diameter larger than 650 nm. Even giant liposomes (1 μm diameter), have retention values < 65% and in fact, the measured last daughter retention for the 650 nm liposomes was found to be substantially lower (11%) than predicted [134,135].

Given the demonstrated robust properties of our peptide capsule design, we have started investigating the delivery of the alpha particle emitting Actinium to cells. To date [198], (in vitro) we have been able to load the BAPCs with ^{225}Ac that have stably retained ≥95% of their activity over 7 days, and shown that cultured

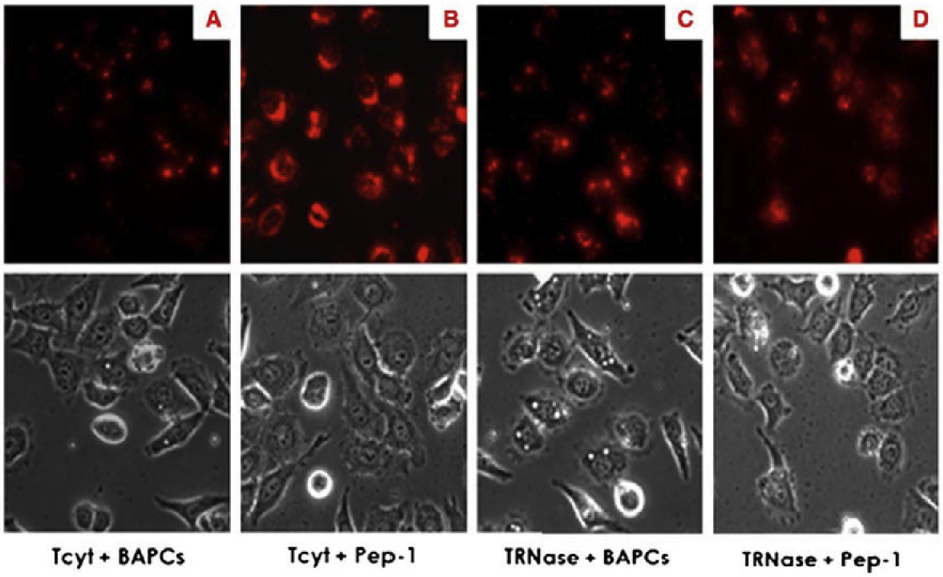

Fig. 19. Fluorescence Microscopy images of BAPCs delivering TAMRA labeled protein to HeLa Cells. A) HeLa cells uptake of BAPCs carrying Tcytc; B) Control with Tcytc with Pep-1; C) BAPCs uptake containing TRNase; D) Control TRNase A with Pep-1. Reproduced from Sukthankar et al. [198].

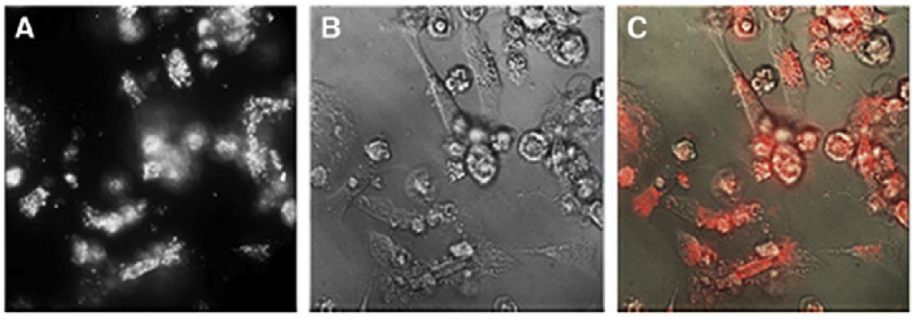

Fig. 20. Time function of the BAPCs integrity. Images obtained with confocal microscopy of BAPC uptake by HeLa cells after 2 weeks showing: A) Excitation of Rhodamine in Dark field image; B) DIC image; C) Merge images exhibiting the Rhodamine inside of the BAPCs. Reproduced from Sukthankar et al. [198].

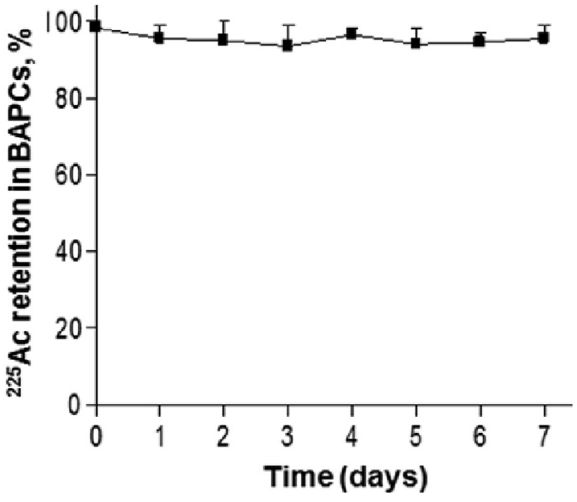

Fig. 21. Retention of BAPCs encapsulated with ^{225}Ac. Encapsulation and retention of ^{225}Ac within BAPCs over 7 days. Reproduced from Sukthankar et al. [198].

cells readily take-up non-lethal concentrations of encapsulated ^{225}Ac. *In vivo* (Fig. 22), free ^{225}Ac completely cleared from the blood while ^{225}Ac-loaded capsules continued to circulate due to their small size.

Free ^{225}Ac accumulated significantly more in the liver ($P = 0.03$) and in the bone ($P = 0.02$) than the ^{225}Ac- BAPCs which points to the tight incorporation of ^{225}Ac inside the BAPCs. At 1 h when both ^{225}Ac-BAPCs and free ^{225}Ac were still exiting the peritoneal cavity there was no significant difference in organ uptake between ^{225}Ac-BAPCs and free ^{225}Ac except for the bone where free ^{225}Ac tends to accumulate. The only organ where there was more ^{213}Bi present compared to ^{225}Ac were kidneys which serve as the “sink” for ^{213}Bi which has been released from any organ in the body.^{213}Bi daughter was present together with ^{225}Ac indicating the possible retention of the daughter by the BAPCs as well. Together, these preliminary results point to the ability of BAPCs to incorporate and retain ^{225}Ac and its daughter ^{213}Bi. Being able to selectively deliver this isotope to a location just outside the nucleus using targeting molecule adducted BAPCs should improve therapeutic efficacy while reducing off-target damage and lowering the whole body dose of radiation needed to kill targeted cells.

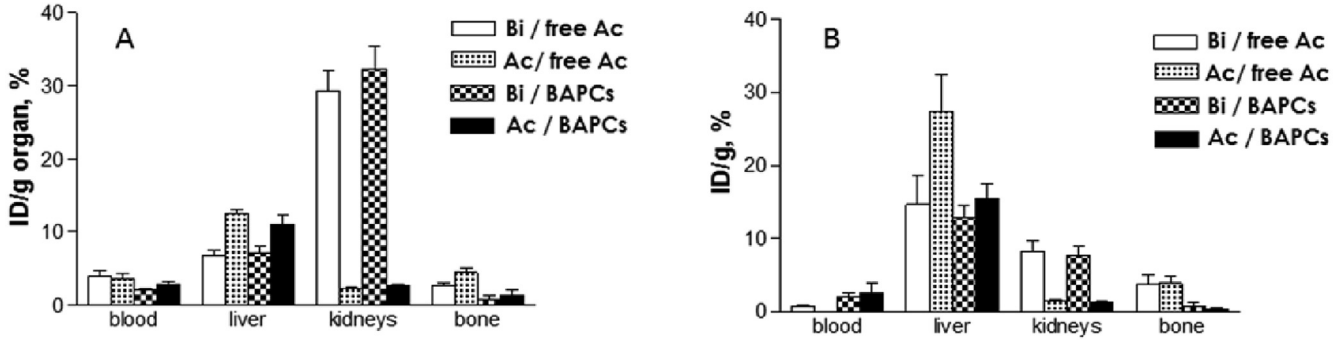

Fig. 22. Biodistribution of free and BAPC-encapsulated, ^{225}Ac and its daughter ^{213}Bi, in CD1 mice. A) 1 h time point; B) 24 h time point. Reproduced from Sukthankar et al. [198].

5. Summary

There are three fundamental factors that go into the development of a competent nano-encapsulating system, viz - characteristics of the diseased state, choice of therapeutics and the nature of the delivery vehicle. The choice of the therapeutic and the nature of its action need to be carefully considered during the selection of a delivery platform. The drug's site and mechanism of action define what carrier system will achieve optimal delivery. For example; drugs that require intracellular sites of action require intracellular delivery for bioactivity and therefore necessitate a delivery vehicle that enables homogenous tissue penetration.

Fundamental research into the nature of diseased state biomarkers and associated ligands, play vital roles in the design of functionalized delivery vehicles. Even in cases where targeting is not employed, an understanding into the characteristics of the diseased site, tissue accumulation and cellular uptake can help us engineer more efficient non-specific drug delivery systems by modulating the biophysical properties of nano-carriers [206,207]. BAPCs by their very nature represent a new and exciting class of novel encapsulating nano-system for drug delivery, not only because of their versatility, tune-ability, extraordinary stability, biocompatibility or target-ability; but also because of the unique structural potentialities of its branched parent sequences that result in the formation of a pure peptide bilayer delimited nano-vesicle similar to liposomes in its organizational architecture. Indeed it could be said that the branched peptide sequences that constitute BAPCs are in themselves a unique class of biomaterial with great potential in a variety of chemical, physical and biological applications. An exhaustive investigation of these nano-materials is currently in progress.

Acknowledgments

We thank Professor Jianhan Chen for carrying out the computer simulation that generated Fig. 16. This is publication **16-158-J** from the Kansas Agricultural Experiment Station. Partial support for this project was provided by PHS-NIH grant # GM074096 and a Terry Johnson Cancer Center Innovation Award (to J.M.T), Scholarship award (to S. B.) from the Coordenação de Aperfeiçoamento de Pessoal de Nível Superior (CAPES) Process number: PDSE - 99999.007690/2014-02, Affilation: CAPES Foundation, Ministry of Education, Brasilia–DF 70.040-020, Brazil and the Terry Johnson Cancer Center at Kansas State University for summer support (for P.S. and S.G.).

References

[1] J. Shi, A.R. Votruba, O.C. Farokhzad, R. Langer, Nanotechnology in drug delivery and tissue engineering: from discovery to applications, ACS Nano Lett. 10 (2010) 3223–3230.
[2] J.K. Kim, H.J. Kim, J.Y. Chung, J.H. Lee, S.B. Young, Y.H. Kim, Natural and synthetic biomaterials for controlled drug delivery, Arch. Pharm. Res. 37 (2014) 60–68.
[3] J.H. Hamman, G.M. Enslin, A.F. Kotze, Oral delivery of peptide drugs: barriers and developments, Bio. Drugs. 19 (2005) 165–177.
[4] R. Pawar, A. Ben-Ari, A.J. Domb, Protein and peptide parenteral controlled delivery, Expert Opin. Biol. Ther. 4 (2004) 1203–1212.
[5] S.K. Sahoo, S. Parveen, J.J. Panda, The present and future of nanotechnology in human health care, Nanomed. NBM. 3 (2007) 20–31.
[6] D.J. Brayden, Controlled release technologies for drug delivery, Drug Discov. Today. 8 (2003) 976–978.
[7] L. Wang, R. Zeng, C. Li, R. Qiao, Self-assembled polypeptide-block-poly(vinylpyrrolidone) as prospective drug-delivery systems, Coll. Surf. B Biointerfaces. 74 (1) (2009) 284–292.
[8] S.M. Moghimi, J. Szebeni, Stealth liposomes and long circulating nanoparticles: critical issues in pharmacokinetics, opsonization and protein-binding properties, Prog. Lipid. Res. 42 (2003) 463–478.
[9] D.H. Levine, P.P. Ghoroghchian, J. Freudenberg, G. Zhang, M.J. Therien, M.I. Greene, D.A. Hammer, R. Murali, Polymersomes: a new multi-functional tool for cancer diagnosis and therapy, Methods. 46 (1) (2008) 25–32.
[10] H. Tanisaka, S. Kizaka-Kondoh, A. Makino, S. Tanaka, M. Hiraoka, S. Kimura, Near-infrared fluorescent labeled peptosome for application to cancer imaging, Bioconjugate Chem. 19 (1) (2008) 109–117.
[11] M. Ferrari, Cancer nanotechnology: opportunities and challenges, Nat. Rev. Cancer 5 (2005) 161–171.
[12] D.A. LaVan, T. McGuire, R. Langer, Small-scale systems for in vivo drug delivery, Nat. Biotechnol. 21 (2003) 1184–1191.
[13] L. Zhang, F.X. Gu, J.M. Chan, A.Z. Wang, R.S. Langer, O.C. Farokhzad, Nanoparticles in medicine: therapeutic applications and developments, Clin. Pharmacol. Ther. 83 (2008) 761–769.
[14] R. Langer, New methods of drug delivery, Science. 249 (1990) 1527–1533.
[15] M.L. Etheridge, S.A. Campbell, A.G. Erdman, C.L. Haynes, S.M. Wolf, J. McCullough, The big picture on nanomedicine: the state of investigational and approved nanomedicine products, Nanomed. NBM. 9 (2013) 1–14.
[16] W.H. Gmeiner, S. Ghosh, Nanotechnology for cancer treatment, Nanotechnol. Rev. 3 (2) (2015) 111–122.
[17] K.M. Gharpure1, S.Y. Wu, C. Li, G. Lopez-Berestein, A.K. Sood, Nanotechnology: future of oncotherapy, Clin. Cancer Res. 21 (14) (2015) 3121–3130.
[18] B. Mishra, B.B. Patel, S. Tiwari, Colloidal nanocarriers: a review on formulation technology, types and applications toward targeted drug delivery, Nanomed. NBM. 6 (2010) 9–24.
[19] F. Alexis, J.W. Rhee, J.P. Richie, A.F. Radovic-Moreno, R. Langer, O.C. Farokhzad, New frontiers in nanotechnology for cancer treatment, Urol. Oncol. 26 (2008) 74–85.
[20] O. Kayser, A. Lemke, N. Hernandez-Trejo, The impact of nanobiotechnology on the development of new drug delivery systems, Curr. Pharm. Biotechnol. 6 (2005) 3–5.
[21] T. Kubik, K. Bogunia-Kubik, M. Sugisaka, Nanotechnology on duty in medical applications, Curr. Pharm. Biotechnol. 6 (2005) 17–33.
[22] H. Devalapally, D. Shenoy, S. Little, R. Langer, A. Mansoor, Poly(ethylene oxide)-modified poly(beta-amino ester) nanoparticles as a pH-sensitive system for tumor-targeted delivery of hydrophobic drugs: part 3. Therapeutic efficacy and safety studies in ovarian cancer xenograft model, Cancer Chemother. Pharmacol. 59 (4) (2006) 477–484.
[23] J.L. Au, S.H. Jang, J. Zheng, C.T. Chen, S. Song, L. Hu, M.G. Wientjes, Determinants of drug delivery and transport to solid tumors, J. Control Release. 74 (2001) 31–46.
[24] G.J. Fetterly, R.M. Straubinger, Pharmacokinetics of paclitaxel-containing liposomes in rats, AAPS PharmSci. 5 (2003) E32.
[25] D. Hoarau, P. Delmas, S. David, E. Roux, J.C. Leroux, Novel long-circulating lipid nanocapsules, Pharm. Res. 21 (2004) 1783–1789.
[26] O.M. Koo, I. Rubinstein, H. Onyuksel, Camptothecin in sterically stabilized

phospholipid micelles: a novel nanomedicine, Nanomedicine 1 (2005) 77–84.
[27] J. Kristl, B. Volk, M. Gasperlin, M. Sentjurc, P. Jurkovic, Effect of colloidal carriers on ascorbyl palmitate stability, Eur. J. Pharm. Sci. 19 (2003) 181–189.
[28] A. Arnedo, J.M. Irache, M. Merodio, M.S. Espuelas Millan, Albumin nanoparticles improved the stability, nuclear accumulation and anticytomegaloviral activity of a phosphodiester oligonucleotide, J. Control Release. 94 (2004) 217–227.
[29] J.A. Zhang, G. Anyarambhatla, L. Ma, S. Ugwu, T. Xuan, T. Sardone, I. Ahmad, Development and characterization of a novel Cremophor EL free liposome-based paclitaxel (LEP-ETU) formulation, Eur. J. Pharm. Biopharm. 59 (2005) 177–187.
[30] N.K. Ibrahim, N. Desai, S. Legha, P. Soon-Shiong, R.L. Theriault, E. Rivera, B. Esmaeli, S.E. Ring, A. Bedikian, G.N. Hortobagyi, J.A. Ellerhorst, Phase I and pharmacokinetic study of ABI-007, a Cremophor-free, protein-stabilized, nanoparticle formulation of paclitaxel, Clin. Cancer Res. 8 (2002) 1038–1044.
[31] T.Y. Kim, D.W. Kim, J.Y. Chung, S.G. Shin, S.C. Kim, D.S. Heo, N.K. Kim, Y.J. Bang, Phase I and pharmacokinetic study of Genexol-PM, a Cremophor-free, polymeric micelle-formulated paclitaxel, in patients with advanced malignancies, Clin. Cancer Res. 10 (2004) 3708–3716.
[32] A. Krishnadas, I. Rubinstein, H. Onyuksel, Sterically stabilized phospholipid mixed micelles: in vitro evaluation as a novel carrier for water-insoluble drugs, Pharmacol. Res. 20 (2003) 297–302.
[33] H. Gelderblom, J. Verweij, K. Nooter, A. Sparreboom, Cremophor EL: the drawbacks and advantages of vehicle selection for drug formulation, Eur. J. Cancer. 37 (2001) 1590–1598.
[34] A.J. ten Tije, J. Verweij, W.J. Loos, A. Sparreboom, Pharmacological effects of formulation vehicles : implications for cancer chemotherapy, Clin. Pharmacokinet. 42 (2003) 665–685.
[35] M.E. Davis, The first targeted delivery of siRNA in humans via a self-assembling, cyclodextrin polymer-based nanoparticle: from concept to clinic, Mol. Pharm. 6 (2009) 659–668.
[36] P. Decuzzi, R. Pasqualini, W. Arap, M. Ferrari, Intravascular delivery of particulate systems: does geometry really matter? Pharmacol. Res. 26 (2009) 235–243.
[37] Y.B. Patil, U.S. Toti, A. Khdair, L. Ma, J. Panyam, Single-step surface functionalization of polymeric nanoparticles for targeted drug delivery, Biomaterials. 30 (2009) 859–866.
[38] B.S. Kim, S.W. Park, P.T. Hammond, Hydrogen-bonding layer-by-layer-assembled biodegradable polymeric micelles as drug delivery vehicles from surfaces, ACS Nano. 2 (2008) 386–392.
[39] R.V. Rughani, J.P. Schneider, Molecular design of beta-hairpin peptides for material construction, MRS Bull. 33 (5) (2008) 530–535.
[40] H.S. Giddi, M.A. Arunagirinathan, J.R. Bellare, Self-assembled surfactant nano-structures important in drug delivery: a review, Indian J. Exp. Bio. 45 (2) (2007) 133–159.
[41] K. Rajagopal, J.P. Schneider, Self-assembling peptides and proteins for nanotechnological applications, Curr. Opin. Struct. Biol. 14 (4) (2004) 480–486.
[42] R.S. Tu, M. Tirrell, Bottom-up design of biomimetic assemblies, Adv. Drug Deliv. Rev. 56 (11) (2004) 1537–1563.
[43] V. Prasad, N. Kumar, P.R. Mishra, Amphiphilic gels as a potential carrier for topical drug delivery, Drug Deliv. 14 (2) (2007) 75–85.
[44] J.H. Fuhrhop, U. Bindig, U. Siggel, Micellar rods and vesicular tubules made of 14'', 16''-diaminoporphyrins, J. Am. Chem. Soc. 115 (23) (1993) 11036–11037.
[45] J.D. Hartgerink, E. Beniash, S.I. Stupp, Peptide-amphiphile nanofibers: a versatile scaffold for the preparation of self-assembling materials, Proc. Natl. Acad. Sci. U. S. A. 99 (8) (2002) 5133–5138.
[46] G. Porte, Giant micelles in ideal solutions. Either rods or vesicles, J. Phys. Chem. 87 (18) (1983) 3541–3550.
[47] S. Chuanoi, Y. Anraku, M. Hori, A. Kishimura, K. Kataoka, Fabrication of polyion complex vesicles with enhanced salt and temperature resistance and their potential applications as enzymatic nanoreactors, Biomacromolecules. 15 (7) (2014) 2389–2397.
[48] M. Johnsson, K. Edwards, Liposomes, disks, and spherical micelles: aggregate structure in mixtures of gel phase phosphatidylcholines and poly(ethylene glycol)-phospholipids, Biophys. J. 85 (6) (2003) 3839–3847.
[49] S.J. Holder, N.A.J.M. Sommerdijk, New micellar morphologies from amphiphilic block copolymers: disks, toroids and bicontinuous micelles, Polym. Chem. 2 (2011) 1018–1028.
[50] A.G. Daful, J.B. Avalos, A.D. Mackie, Model shape transitions of micelles: spheres to cylinders and disks, Langmuir 28 (8) (2012) 3730–3743.
[51] H. Honggang Cui, T.K. Hodgdon, E.W. Kaler, L. Abezgauz, D. Danino, M. Lubovsky, Y. Talmond, D.J. Pochan, Elucidating the assembled structure of amphiphiles in solution via cryogenic transmission electron microscopy, Soft Matter 3 (2007) 945–955.
[52] A. Trent, R. Marullo, B. Lin, M. Black, M. Tirrell, Structural properties of soluble peptide amphiphile micelles, Soft Matter 7 (2011) 9572–9582.
[53] S. dos Santos, B. Medronho, T. dos Santos, F.E. Antunes, Amphiphilic molecules in drug delivery systems, in: J. Coelho (Ed.), Drug Delivery Systems: Advanced Technologies Potentially Applicable in Personalised Treatment, Advances in Predictive, Preventive and Personalised Medicine, Springer Science and Business Media, Dordrecht, Netherlands, 2013, pp. 35–85.
[54] C.J. Drummond, C. Fong, Surfactant self-assembly objects as novel drug delivery vehicles, Curr. Opin. Colloid Interface Sci. 4 (6) (1999) 449–456.
[55] A.S. Goldstein, A.N. Lukyanov, P.A. Carlson, P. Yager, M.H. Gelb, Formation of high-axial-ratio-microstructures from natural and synthetic sphingolipids, Chem. Phys. Lipids. 88 (1) (1997) 21–36.
[56] J. Israelachvili, Intermolecular and Surface Forces, third ed., Academic Press, New York, 2011.
[57] K. Letchford, H. Burt, A review of the formation and classification of amphiphilic block copolymer nanoparticulate structures: micelles, nanospheres, nanocapsules and polymersomes, Eur. J. Pharm. Biopharm. 65 (2007) 259–269.
[58] K. Yu, A. Eisenberg, Bilayer morphologies of self-assembled crew-cut aggregates of amphiphilic PS-b-PEO diblock copolymers in solution, Macromolecules 31 (11) (1998) 3509–3518.
[59] M.-S. Hsiao, S.F.M. Yusoff, M.A. Winnik, I. Manners, Crystallization-driven self-assembly of block copolymers with a short crystallizable core-forming segment: controlling micelle morphology through the influence of molar mass and solvent selectivity, Macromolecules 47 (7) (2014) 2361–2372.
[60] H. Shen, L. Zhang, A. Eisenberg, Multiple pH-Induced morphological changes in aggregates of polystyrene-block-poly(4-vinylpyridine) in DMF/H_2O mixtures, J. Am. Chem. Soc. 121 (1999) 2728–2740.
[61] A. Choucair, A. Eisenberg, Interfacial solubilization of model amphiphilic molecules in block copolymer micelles, J. Am. Chem. Soc. 125 (2003) 11993–12000.
[62] A. Choucair, A. Eisenberg, Control of amphiphilic block copolymer morphologies using solution conditions, Eur. Phys. J. E. Soft Matter 10 (2003) 37–44.
[63] J.-F. Le Meins, O. Sandre, S. Lecommandoux, Recent trends in the tuning of polymersomes' membrane properties, Eur. Phys. J. E. Soft Matter 34 (14) (2011) 1–17.
[64] E.P. Holowka, D.J. Pochan, T.J. Deming, Charged polypeptide vesicles with controllable diameter, J. Am. Chem. Soc. 127 (2005) 12423–12428.
[65] G. Cai, H. Zhang, P. Liu, L. Wang, H. Jiang, Triggered disassembly of hierarchically assembled onion-like micelles into the pristine core-shell micelles via a small change in pH, Acta Biomater. 7 (10) (2011) 3729–3737.
[66] E.S. Read, S.P. Armes, Recent advances in shell cross-linked micelles, Chem. Commun. (Camb). 29 (2007) 3021–3035.
[67] R. Erhardt, A. Böker, H. Zettl, H. Kaya, W. Pyckhout-Hintzen, G.V. Krausch, A. Abetz, H.E. Müller, Janus micelles, Macromolecules 34 (4) (2001) 1069–1075.
[68] R. Erhardt, M. Zhang, A. Böker, H. Zettl, C. Abetz, P. Frederik, G. Krausch, V. Abetz, A.X.E. Müller, Amphiphilic janus micelles with polystyrene and poly(methacrylic acid) hemispheres, J. Am. Chem. Soc. 125 (11) (2003) 3260–3267.
[69] I.K. Voets, A. de Keizer, P. de Waard, P.M. Frederik, P.H. Bomans, H. Schmalz, A. Walther, S.M. King, F.A.M. Leermakers, M.A.C. Stuart, Double-faced micelles from water-soluble polymers, Angew. Chem. Int. Ed. Engl. 45 (40) (2006) 6673–6676.
[70] V. Bütün, S. Liu, J.V.M. Weaver, X. Bories-Azeau, Y. Cai, S.P. Armes, A brief review of 'schizophrenic' block copolymers, React. Funct. Polym. 66 (1) (2006) 157–165.
[71] Z. Li, M.A. Hillmyer, T.P. Lodge, Control of structure in multicompartment micelles by blending μ-ABC star terpolymers with AB diblock copolymers, Macromolecules. 39 (2) (2006) 765–771.
[72] V.P. Torchilin, Recent advances with liposomes as pharmaceutical carriers, Nat. Rev. Drug Discov. 4 (2005) 145–160.
[73] G.S. Kwon, Polymeric micelles for delivery of poorly water-soluble compounds, Crit. Rev. Ther. Drug Carr. Syst. 20 (2003) 357–403.
[74] A. Vonarbourg, C. Passirani, P. Saulnier, J.P. Benoit, Parameters influencing the stealthiness of colloidal drug delivery systems, Biomaterials. 27 (2006) 4356–4373.
[75] G. Henriksen, B.W. Schoultz, T.E. Michaelsen, Ø.S. Bruland, R.H. Larsen, Sterically stabilized liposomes as a carrier for á-emitting radium and actinium radionuclides, Nucl. Med. Biol. 31 (2004) 441–449.
[76] M. Miederer, D.A. Scheinberg, M.R. McDevitt, Realizing the potential of the actinium-225 radionuclide generator in targeted alpha particle therapy applications, Adv. Drug Deliv. Rev. 60 (2008) 1371–1382.
[77] H. Takeuchi, H. Kojima, H. Yamamoto, Y. Kawashima, Evaluation of circulation profiles of liposomes coated with hydrophilic polymers having different molecular weights in rats, J. Control. Release 75 (2001) 83–91.
[78] D. Garrec, M. Ranger, J. Leroux, Micelles in anticancer drug delivery, Am. J. Drug Deliv. 2 (2004) 15–42.
[79] E.S. Lee, K. Na, Y.H. Bae, Polymeric micelle for tumor pH and folate-mediated targeting, J. Control Release. 91 (2003) 103–113.
[80] E.S. Lee, K. Na, Y.H. Bae, Doxorubicin loaded pH-sensitive polymeric micelles for reversal of resistant MCF-7 tumor, J. Control Release. 103 (2005) 405–418.
[81] Y. Matsumura, T. Hamaguchi, T. Ura, K. Muro, Y. Yamada, Y. Shimada, K. Shirao, T. Okusaka, H. Ueno, M. Ikeda, N. Watanabe, Phase I clinical trial and pharmacokinetic evaluation of NK911, a micelle-encapsulated doxorubicin, Br. J. Cancer 91 (2004) 1775–1781.
[82] A. Nagai, Y. Nagai, H. Qu, S. Zhang, Dynamic behaviors of lipid-like self-assembling peptide A6D and A6K nanotubes, J. Nanosci. Nanotechnol. 7 (2) (2007) 2246–2252.
[83] A.S. Ojugo, P.M. McSheehy, D.J. McIntyre, C. McCoy, M. Stubbs, M.O. Leach, I.R. Judson, J.R. Griffiths, Measurement of the extracellular pH of solid

tumours in mice by magnetic resonance spectroscopy: a comparison of exogenous (19)F and (31)P probes, NMR Biomed. 12 (1999) 495–504.
[84] K. Engin, D.B. Leeper, J.R. Cater, A.J. Thistlethwaite, L. Tupchong, J.D. McFarlane, Extracellular pH distribution in human tumours, Int. J. Hyperth. 11 (1995) 211–216.
[85] H. Wu, L. Zhu, V.P. Torchilin, pH-sensitive poly(histidine)-PEG/DSPE-PEG co-polymer micelles for cytosolic drug delivery, Biomaterials 34 (2013) 1213–1222.
[86] A. Lavasanifar, J. Samuel, G.S. Kwon, Poly(ethylene oxide)-block-poly(L-amino acid) micelles for drug delivery, Adv. Drug Deliv. Rev. 54 (2002) 169–190.
[87] Y. Li, G.S. Kwon, Methotrexate esters of poly(ethylene oxide)-block-poly(2-hydroxyethyl-L-aspartamide). Part I: effects of the level of methotrexate conjugation on the stability of micelles and on drug release, Pharm. Res. 17 (2000) 607–611.
[88] Y. Bae, N. Nishiyama, S. Fukushima, H. Koyama, M. Yasuhiro, K. Kataoka, Preparation and biological characterization of polymeric micelle drug carriers with intracellular pH-triggered drug release property: tumor permeability, controlled subcellular drug distribution, and enhanced in vivo antitumor efficacy, Bioconjug. Chem. 16 (2005) 122–130.
[89] A. Graciaa, M. Ben Ghoulam, G. Marion, J.J. Lachaise, Critical concentrations and compositions of mixed micelles of sodium dodecylbenzenesulfonate, tetradecyltrimethylammonium bromide, and polyoxyethylene octylphenols, J. Phys. Chem. 93 (1989) 4167–4173.
[90] Z.J. Yu, G.X. Zhao, Micellar compositions in mixed surfactant solutions, J. Colloid Interface Sci. 156 (2) (1993) 325–328.
[91] M. Ishikawa, K. Matsumura, K. Esumi, K. Meguro, Mixed micelle formation between anionic surfactant and α,ω-type cationic surfactant in aqueous solutions: sodium dodecyl sulfate and N,N'-1,12-dodecanediylbis(triethylammonium bromide) system, J. Colloid Interface Sci. 141 (1) (1991) 10–20.
[92] C. Tanford, The Hydrophobic Effect Formation of Micelles and Biological Membranes, Wiley-Interscience NY, NY, 1980.
[93] P. Jokela, B. Joensson, A. Khan, Phase equilibria of catanionic surfactant-water systems, J. Phys. Chem. 91 (1987) 3291–3298.
[94] E.W. Kaler, A.K. Murthy, B.E. Rodriguez, J.A. Zasadzinski, Spontaneous vesicle formation in aqueous mixtures of single-tailed surfactants, Science 245 (4924) (1989) 1371–1374.
[95] R.H. Müller, K. Mäder, S. Gohla, Solid lipid nanoparticles (SLN) for controlled drug delivery – a review of the state of the art, Eur. J. Pharm. Biopharm. 50 (2000) 161–177.
[96] I.P. Kaur, R. Bhandari, S. Bhandari, V. Kakkar, Potential of solid lipid nanoparticles in brain targeting, J. Control Release. 127 (2008) 97–109.
[97] P. Blasi, S. Giovagnoli, A. Schoubben, M. Ricci, C. Rossi, Solid lipid nanoparticles for targeted brain drug delivery, Adv. Drug Deliv. Rev. 59 (2007) 454–477.
[98] G.P. Zara, R. Cavalli, A. Bargoni, A. Fundaro, D. Vighetto, M.R. Gasco, Intravenous administration to rabbits of non-stealth and stealth doxorubicin-loaded solid lipid nanoparticles at increasing concentrations of stealth agent: pharmacokinetics and distribution of doxorubicin in brain and other tissues, J. Drug Target. 10 (2002) 327–335.
[99] A. Sinaga, T.A. Hatton, K.C. Tam, Poly(acrylic acid)-block-poly(L-valine): evaluation of beta-sheet formation and its stability using circular dichroism technique, Biomacromolecules 8 (9) (2007) 2801–2808.
[100] S.A. Wissing, O. Kayser, R.H. Muller, Solid lipid nanoparticles for parenteral drug delivery, Adv. Drug Deliv. Rev. 56 (2004) 1257–1272.
[101] A. Quintana, E. Raczka, L. Piehler, I. Lee, A. Myc, I. Majoros, A.K. Patri, T. Thomas, J. Mule, J.R. Baker Jr., Design and function of a dendrimer-based therapeutic nano-device targeted to tumor cells through the folate receptor, Pharm. Res. 19 (2002) 1310–1316.
[102] U. Boas, P.M. Heegaard, Dendrimers in drug research, Chem. Soc. Rev. 33 (2004) 43–63.
[103] R.M. Mainardes, L.P. Silva, Drug delivery systems: past, present, and future, Curr. Drug Targets. 5 (2004) 449–455.
[104] A. Carlmark, C. Hawker, A. Hult, M. Malkoch, New methodologies in the construction of dendritic molecules, Chem. Soc. Rev. 38 (2008) 352–362.
[105] M.J. Cloninger, Biological applications of dendrimers, Curr. Opin. Chem. Biol. 6 (2002) 742–748.
[106] V. Percec, D.A. Wilson, P. Leowanawat, C.J. Wilson, A.D. Hughes, M.S. Kaucher, D.A. Hammer, D.H. Levine, A.J. Kim, F.S. Bates, K.P. Davis, T.P. Lodge, M.L. Klein, R.H. DeVane, E. Aqad, B.M. Rosen, A.O. Argintaru, M.J. Sienkowska, K. Rissanen, S. Nummelin, J. Ropponen, Self-assembly of janus dendrimers into uniform dendrimersomes and other complex architectures, Science. 328 (5981) (2010) 1009–1014.
[107] J. Ropponen, S. Nummelin, K. Rissanen, Bisfunctionalized janus molecules, Org. Lett. 6 (15) (2004) 2495–2497.
[108] B.M. Rosen, C.J. Wilson, D.A. Wilson, M. Peterca, M.R. Imam, V. Percec, Dendron-mediated self-assembly, disassembly, and self-organization of complex systems, Chem. Rev. 109 (11) (2009) 6275–6540.
[109] P.K. Tripathi, A.J. Khopade, S. Nagaich, S. Shrivastava, S. Jain, N.K. Jain, Dendrimer grafts for delivery of 5-fluorouracil, Pharmazie. 57 (2002) 261–264.
[110] A.S. Chauhan, N.K. Jain, P.V. Diwan, A.J. Khopade, Solubility enhancement of indomethacin with poly(amidoamine) dendrimers and targeting to inflammatory regions of arthritic rats, J. Drug Target. 12 (2004) 575–583.
[111] M. El-Sayed, M.F. Kiani, M.D. Naimark, A.H. Hikal, H. Ghandehari, Extravasation of poly(amidoamine) (PAMAM) dendrimers across microvascular network endothelium, Pharm. Res. 18 (2001) 23–28.
[112] R. Jevprasesphant, J. Penny, R. Jalal, D. Attwood, N.B. McKeown, A. D'Emanuele, The influence of surface modification on the cytotoxicity of PAMAM dendrimers, Int. J. Pharm. 252 (2003) 263–266.
[113] S.S. Nigavekar, L.Y. Sung, M. Llanes, A. El-Jawahri, T.S. Lawrence, C.W. Becker, L. Balogh, M.K. Khan, 3H dendrimer nanoparticle organ/tumor distribution, Pharm. Res. 21 (2004) 476–483.
[114] F.E. Antunes, E.F. Marques, M.G. Miguel, B. Lindman, Polymer-vesicle association, Adv. Colloid Interface Sci. 147–148 (2009) 18–35.
[115] M.A. Moses, H. Brem, R. Langer, Advancing the field of drug delivery: taking aim at cancer, Cancer Cell 4 (2003) 337–341.
[116] A. Samad, Y. Sultana, M. Aqil, Liposomal drug delivery systems: an update review, Curr. Drug Deliv. 4 (2007) 297–305.
[117] S.L. Hart, Lipid carriers for gene therapy, Curr. Drug Deliv. 2 (2005) 423–428.
[118] M.A. Moses, H. Brem, R. Langer, Advancing the field of drug delivery: taking aim at cancer, Cancer Cell 4 (2003) 337–341.
[119] T.M. Allen, P.R. Cullis, Drug delivery systems: entering the mainstream, Science 303 (2004) 1818–1822.
[120] S. Ning, Q. Huang, X. Sun, C. Li, Y. Zhang, J. Li, Y.-N. Liu, Carboxymethyl dextran-coated liposomes: toward a robust drug delivery platform, Soft Matter 7 (2011) 9394–9401.
[121] H.R. Marsden, I. Tomatsua, A. Kros, Model systems for membrane fusion, Chem. Soc. Rev. 40 (2011) 1572–1585.
[122] K. Ewert, H.M. Evans, A. Ahmad, N.L. Slack, A.J. Lin, A. Martin-Herranz, C.R. Safinya, Lipoplex structures and their distinct cellular pathways, Adv. Genet. 53 (2005) 119–155.
[123] S. Pollock, R. Antrobus, R. Newton, B. Kampa, J. Rossa, S. Latham, N.B. Nichita, R.A. Dwek, N. Zitzmann, Uptake and trafficking of liposomes to the endoplasmic reticulum, FASEB J. 24 (6) (2010) 1866–1878.
[124] T.M. Allen, A. Chonn, Large unilamellar liposomes with low uptake into the reticuloendothelial system, FEBS Lett. 223 (1987) 42–46.
[125] S. Ning, Q. Huang, X. Sun, C. Li, Y. Zhang, J. Li, Y.-N. Liu, Carboxymethyl dextran-coated liposomes: toward a robust drug delivery platform, Soft Matter 7 (2011) 9394–9401.
[126] A. Chonn, P.R. Cullis, Ganglioside GM1 and hydrophilic polymers increase liposome circulation times by inhibiting the association of blood proteins, J. Liposome Res. 2 (3) (1992) 397–410.
[127] H. Takeuchi, H. Yamamoto, T. Toyoda, H. Toyobuku, T. Hino, Y. Kawashima, Physical stability of size controlled small unilameller liposomes coated with a modified polyvinyl alcohol, Int. J. Pharm. 164 (1998) 103–111.
[128] M.L. Immordino, F. Dosio, L. Cattel, Stealth liposomes: review of the basic science, rationale, and clinical applications, existing and potential, Int. J. Nanomed. 1 (3) (2006) 297–315.
[129] S.H. Jung, S. Jung, H. Seong, S.H. Cho, K.S. Jeong, B.C. Shin, Polyethylene glycol-complexed cationic liposome for enhanced cellular uptake and anticancer activity, Int. J. Pharm. 382 (1–2) (2009) 254–261.
[130] V.P. Torchilin, T.S. Levchenko, K.R. Whiteman, A.A. Yaroslavov, A.M. Tsatsakis, A.K. Rizos, E.V. Michailova, M.I. Shtilman, Amphiphilic poly-N-vinylpyrrolidones: synthesis, properties and liposome surface modification, Biomaterials 22 (2001) 3035–3044.
[131] D.B. Kirpotin, D.C. Drummond, Y. Shao, M.R. Shalaby, K. Hong, U.B. Nielsen, J.D. Marks, C.C. Benz, J.W. Park, Antibody targeting of long-circulating lipidic nanoparticles does not increase tumor localization but does increase internalization in animal models, Cancer Res. 66 (2006) 6732–6740.
[132] M.T. Basel, T.B. Shrestha, D.L. Troyer, S.H. Bossmann, Protease-sensitive, polymer-caged liposomes: a method for making highly targeted liposomes using triggered release, ACS Nano. 5 (3) (2011) 2162–2175.
[133] Y.S. Kim, M.W. Brechbiel, An overview of targeted alpha therapy, Tumour Biol. 33 (2012) 573–590.
[134] S. Sofou, J.L. Thomas, H.Y. Lin, M.R. McDevitt, D.A. Scheinberg, G. Sgouros, Engineered liposomes for potential alpha-particle therapy of metastatic cancer, J. Nucl. Med. 45 (2004) 253–260.
[135] S. Sofou, B.J. Kappel, J.S. Jaggi, M.R. McDevitt, D.A. Scheinberg, G. Sgouros, Enhanced retention of the alpha-particle-emitting daughters of actinium-225 by liposome carriers, Bioconjug. Chem. 18 (2007) 2061–2067.
[136] O. Sartor, Radioisotopic treatment of bone pain from metastatic prostate cancer, Curr. Oncol. Rep. 5 (2003) 258–262.
[137] M. Hamoudeh, M.A. Kamleh, R. Diab, H. Fessi, Radionuclides delivery systems for nuclear imaging and radiotherapy of cancer, Adv. Drug Deliv. Rev. 60 (2008) 1329–1346.
[138] O.M. Koo, I. Rubinstein, H. Onyuksel, Role of nanotechnology in targeted drug delivery and imaging: a concise review, Nanomed. NBM. 1 (2005) 193–212.
[139] A.A. Gabizon, H. Shmeeda, S. Zalipsky, Pros and cons of the liposome platform in cancer drug targeting, J. Liposome Res. 16 (2006) 175–183.
[140] T.M. Allen, L.G. Cleland, Serum-induced leakage of liposome contents, Biochem. Biophys. Acta Biomembr. 597 (1980) 418–426.
[141] V.K. Moyrya, N.N. Inamdar, Trimethyl chitosan and its applications in drug delivery, J. Mater. Sci. Mater. Med. 20 (5) (2009) 1057–1079.
[142] H.Y. Nam, S.M. Kwon, H. Chung, S.-Y. Lee, S.-H. Kwon, H. Jeon, Y. Kim, J.H. Park, J. Kim, S. Her, Y.-K. Oh, I.C. Kwon, K. Kim, S.Y. Jeong, Hydrophobically modified glycol chitosan nanoparticles-encapsulated camptothecin enhance the drug stability and tumor targeting in cancer therapy, J. Control Release 127 (3) (2008) 208–218.
[143] P.S. Pramod, R. Shah, S. Chaphekar, N. Balasubramanian, M. Jayakannan, Polysaccharide nano-vesicular multidrug carriers for synergistic killing of

cancer cells, Nanoscale 6 (2014) 11841–11855.
[144] P.S. Pramod, R. Shah, M. Jayakannan, Dual stimuli polysaccharide nanovesicles for conjugated and physically loaded doxorubicin delivery in breast cancer cells, Nanoscale 7 (2015) 6636–6652.
[145] V.K. Moyrya, N.N. Inamdar, Trimethyl chitosan and its applications in drug delivery, J. Mater. Sci. Mater. Med. 20 (5) (2009) 1057–1079.
[146] H.Y. Nam, S.M. Kwon, H. Chung, S.-Y. Lee, S.-H. Kwon, H. Jeon, Y. Kim, J.H. Park, J. Kim, S. Her, Y.-K. Oh, I.C. Kwon, K. Kim, S.Y. Jeong, Hydrophobically modified glycol chitosan nanoparticles-encapsulated camptothecin enhance the drug stability and tumor targeting in cancer therapy, J. Control Release 127 (3) (2008) 208–218.
[147] I.F. Uchegbu, S.P. Vyas, Non-ionic surfactant based vesicles (niosomes) in drug delivery, Int. J. Pharm. 172 (1998) 33–70.
[148] G. Vanlerberghe, R.M. Handjani-Vila, A. Ribier, Les niosomes, une nouvelle famille de vesicules a' base d'amphiphiles non ioniques, in: Physicochimie des compose's amphiphiles. Coll. Nat, CNRS. Editions du CNRS, Paris, 1978, pp. 303–311.
[149] R.M. Handjani-Vila, A. Ribier, B. Rondot, G. Vanlerberghie, Dispersions of lamellar phases of non-ionic lipids in cosmetic products, Int. J. Cosmet. Sci. 1 (5) (1979) 303–314.
[150] Handjani-Vila, R. M., Guy, V. (1975) Procédé de fabrication de dispersions aqueuses de spérules lipidiques et nouvelles compositions correspondantes, L'Oréal, French Patent 2315991–A1.
[151] Handjani-Vila, R. M., Ribier, A.,, Vanlerberghie, G, Zabotto, A., Griat, J. (1989) Cosmetic and pharmaceutical compositions containing niosomes and a water-soluble polyamide, and a process for preparing these compositions, L'Oréal, U. S. Patent No. 4830857.
[152] T. Yoshioka, B. Sternberg, A.T. Florence, Preparation and properties of vesicles (niosomes) of sorbitan monoesters (span 20, 40, 60 and 80) and a sorbitan triester (span 85), Int. J. Pharm. 105 (1) (1994) 1–6.
[153] K.M. Kazi, A.S. Mandal, N. Biswas, A. Guha, S. Chatterjee, M. Behera, K. Kuotsu, Niosome: a future of targeted drug delivery systems, J. Adv. Pharm. Technol. Res. 1 (2010) 374–380.
[154] C. Marianecci, L. Di Marzio, F. Rinaldi, C. Celia, D. Paolino, F. Alhaique, S. Esposito, M. Carafa, Niosomes from 80s to present: the state of the art, Adv. Colloid Interface Sci. 205 C (2013) 187–206.
[155] C. Hu, D.G. Rhodes, Proniosomes: a novel drug carrier preparation, Int. J. Pharm. 185 (1999) 23–35.
[156] V.R. Yasam, S.L. Jakki, J. Natarajan, G. Kuppusamy, A review on novel vesicular drug delivery: proniosomes, Drug Deliv. 21 (4) (2014) 243–249.
[157] J.Y. Fang, C.T. Hong, W.T. Chiu, Y.Y. Wang, Effect of liposomes and niosomes on skin permeation of enoxacin, Int. J. Pharm. 219 (2001) 61–72.
[158] M. Manconi, C. Sinico, D. Valenti, F. Lai, A.M. Fadda, Niosomes as carriers for tretinoin. III. A study into the in vitro cutaneous delivery of vesicle-incorporated tretinoin, Int. J. Pharm. 311 (2006) 11–19.
[159] M. Carafa, C. Marianecci, F. Rinaldi, E. Santucci, S. Tampucci, D. Monti, Span and tween neutral and pH-sensitive vesicles: characterization and in vitro skin permeation, J. Liposome Res. 19 (2009) 332–340.
[160] D.A. Hajduk, M.B. Kossuth, M.A. Hillmyer, F.S. Bates, Complex phase behavior in aqueous solutions of poly(ethylene oxide)-Poly(ethylethylene) block copolymers, J. Phys. Chem. B 102 (22) (1998) 4269–4276.
[161] H.E. Warriner, S.H. Idziak, N.L. Slack, P. Davidson, C.R. Safinya, Lamellar biogels: fluid-membrane-based hydrogels containing polymer lipids, Science 271 (5251) (1996) 969–973.
[162] F. Meng, Z. Zhong, J. Feijen, Stimuli-responsive polymersomes for programmed drug delivery, Biomacromolecules. 10 (2) (2009) 197–209.
[163] D. Needham, D.V. Zhelev, in: M. Rosoff (Ed.), The Mechanochemistry of Lipid Vesicles Examined by Micropipette Manipulation Techniques in Vesicles, Marcel Dekker, New York, 2000. Ch. 9.
[164] G. Srinivas, D.E. Discher, M.L. Klein, Self-assembly and properties of diblock copolymers by coarse-grain molecular dynamics, Nat. Mater. 3 (9) (2004) 638–644.
[165] H. Hu, M. Gopinadhan, C.O. Osuji, Directed self-assembly of block copolymers: a tutorial review of strategies for enabling nanotechnology with soft matter, Soft Matter 10 (2014) 3867–3889.
[166] Y. Mai, A. Eisenberg, Self-assembly of block copolymers, Chem. Soc. Rev. 41 (2012) 5969–5985.
[167] S. Santoso, W. Hwang, H. Hartman, S. Zhang, Self-assembly of surfactant-like peptides with variable glycine tails to form nanotubes and nanovesicles, Nano Lett. 2 (7) (2002) 687–691.
[168] G. Von Maltzahn, S. Vauthey, S. Santoso, S. Zhang, Positively charged surfactant-like peptides self-assemble into nanostructures, Langmuir 19 (10) (2003) 4332–4337.
[169] H. Xu, J. Wang, S. Han, J. Wang, D. Yu, H. Zhang, D. Xia, X. Zhao, T.A. Waigh, J.R. Lu, Hydrophobic-region-induced transitions in self-assembled peptide nanostructures, Langmuir. 25 (7) (2009) 4115–4123.
[170] S.J. Yang, S. Zhang, Self-assembling behavior of designer lipid-like peptides, Supramol. Chem. 18 (5) (2006) 389–396.
[171] X. Zhao, F. Pan, S. Perumal, H. Xu, J.R. Lu, J.R.P. Webster, Interfacial assembly of cationic peptide surfactants, Soft Matter. 5 (8) (2009) 1630–1638.
[172] S. Vauthey, S. Santoso, H. Gong, N. Watson, S. Zhang, Molecular self-assembly of surfactant-like peptides to form nanotubes and nanovesicles, Proc. Natl. Acad. Sci. U.S.A. 99 (2002) 5355–5360.
[173] S. Tsonchev, A. Troisi, G.C. Schatz, M.A. Ratner, On the structure and stability of self-assembled zwitterionic peptide amphiphiles: a Theoretical study, Nano Lett. 4 (3) (2004) 427–431.
[174] S. Santoso, W. Hwang, H. Hartman, S. Zhang, Self-assembly of surfactant-like peptides with variable glycine tails to form nanotubes and nanovesicles, Nano Lett. 2 (2002) 687–691.
[175] X. Zhao, F. Pan, H. Xu, M. Yaseen, H. Shan, C.A. Hauser, S. Zhang, J.R. Lu, Molecular self-assembly and applications of designer peptide amphiphiles, Chem. Soc. Rev. 39 (9) (2010) 3480–3498.
[176] W. Jeong, Y. Lim, Macrocyclic peptides self-assemble into robust vesicles with molecular recognition capabilities, Bioconjug. Chem. 25 (2014) 1996–2003.
[177] D. Jiao, J. Geng, X.J. Loh, D. Das, T.-C. Lee, O.A. Sherman, Supramolecular peptide amphiphile vesicles through host–guest complexation, Angew. Chem. Int. Ed. Engl. 51 (2012) 9633–9637.
[178] X.J. Loh, J. del Barrio, T.-C. Lee, O.A. Sherman, Supramolecular polymeric peptide amphiphile vesicles for the encapsulation of basic fibroblast growth factor, Chem. Commun. 50 (2014) 3033–3035.
[179] A.J. van Hell, C.I.C.A. Costa, F.M. Flesch, M. Sutter, W. Jiskoot, D.J.A. Crommelin, W.E. Hennink, E. Mastrobattista, Self-Assembly of Recombinant Amphiphilic Oligopeptides into Vesicles, Biomacromolecules. 8 (2007) 2753–2761.
[180] A.J. van Hell, M.M. Fretz, D.J.A. Crommelin, W.E. Hennink, E. Mastrobattista, Peptide nanocarriers for intracellular delivery of photosensitizers, J. Control Release. 141 (3) (2010) 347–353.
[181] M. Rad-Malekshahi, K.M. Visscher, J.P. Rodrigues, R. de Vries, W.E. Hennink, M. Baldus, A.M. Bonvin, E. Mastrobattista, M. Weingarth, The supramolecular organization of a peptide-based nanocarrier at high molecular detail, J. Am. Chem. Soc. 137 (2015) 7775–7784.
[182] S. Zhang, Emerging biological materials through molecular self-assembly, Biotechnol. Adv. 20 (5–6) (2002) 321–339.
[183] D.J. Adams, D. Atkins, A.I. Cooper, S. Furzeland, A. Trewin, I. Young, Vesicles from peptidic side-chain polymers synthesized by atom transfer radical polymerization, Biomacromolecules 9 (11) (2008) 2997–3003.
[184] S. Gudlur, P. Sukthankar, J. Gao, L.A. Avila, Y. Hiromasa, J. Chen, T. Iwamoto, J.M. Tomich, Peptide nanovesicles formed by the self-assembly of branched amphiphilic peptides, PLoS One 7 (2012) e45374.
[185] H. Iatrou, H. Frielinghaus, S. Hanski, N. Ferderigos, J. Ruokolainen, O. Ikkala, D. Richter, J. Mays, N. Hadjichristidis, Architecturally induced multiresponsive vesicles from well-defined polypeptides: formation of gene vehicles, Biomacromolecules 8 (7) (2007) 2173–2181.
[186] S. Kar, M.G. Drew, A. Pramanik, Formation of vesicles through solvent assisted self-assembly of hydrophobic pentapeptides: encapsulation and pH responsive release of dyes by the vesicles, Protein Pept. Lett. 18 (9) (2011) 886–897.
[187] K.E. Gebhardt, S. Ahn, G. Venkatachalam, D.A. Savin, Role of secondary structure changes on the morphology of polypeptide-based block copolymer vesicles, J. Colloid Interface Sci. 317 (1) (2008) 70–76.
[188] J. Sun, X. Chen, T. Lu, S. Liu, H. Tian, Z. Guo, X. Jing, Formation of reversible shell cross-linked micelles from the biodegradable amphiphilic diblock copolymer poly(L-cysteine)-block-poly(L-lactide), Langmuir. 24 (18) (2008) 10099–10106.
[189] R.E. Sallach, M. Wei, N. Biswas, V.P. Conticello, S. Lecommandoux, R.A. Dluhy, E.L. Chaikof, Micelle density regulated by a reversible switch of protein secondary structure, J. Am. Chem. Soc. 128 (36) (2006) 12014–12019.
[190] Y.S. Velichko, S.I. Stupp, M.O. de la Cruz, Molecular simulation study of peptide amphiphile self-assembly, J. Phys. Chem. B 112 (8) (2008) 2326–2334.
[191] X. Shen, X. Mo, R. Moore, S.J. Frazier, T. Iwamoto, J.M. Tomich, X.S. Sun, Adhesion and structure properties of protein nanomaterials containing hydrophobic and charged amino acids, J. Nanosci. Nanotechnol. 6 (3) (2006) 837–844.
[192] X. Mo, Y. Hiromasa, M. Warner, A.N. Al-Rawi, T. Iwamoto, T.S. Rahman, X. Sun, J.M. Tomich, Design of 11-residue peptides with unusual biophysical properties: induced secondary structure in the absence of water, Biophys. J. 945 (2008) 1807–1817.
[193] A. Grove, J.M. Tomich, T. Iwamoto, M. Montal, Design of a functional calcium channel protein: inferences about an ion channel-forming motif derived from the primary structure of voltage-gated calcium channels, Protein Sci. 2 (11) (1993) 1918–1930.
[194] T. Iwamoto, A. Grove, M.O. Montal, M. Montal, J.M. Tomich, Chemical synthesis and characterization of peptides and oligomeric proteins designed to form transmembrane ion channels, Int. J. Pept. Protein Res. 43 (6) (1994) 597–607.
[195] P. Sukthankar, S. Gudlur, L.A. Avila, S. Whitaker, B.B. Katz, Y. Hiromasa, J. Gao, P. Thapa, D. Moore, T. Iwamoto, J.M. Tomich, Branched oligopeptides form nano-capsules with lipid vesicle characteristics, Langmuir 29 (2013) 14648–14654.
[196] P. Sukthankar, S.K. Whitaker, M. Garcia, A. Herrera, M. Boatwright, O. Prakash, J.M. Tomich, Thermally induced conformational transitions in nascent branched amphiphilic peptide capsules, Langmuir 31 (10) (2015) 2946–2955.
[197] R.L. Biltonen, D. Lichtenberg, The use of differential scanning calorimetry as a tool to characterize liposome preparations, Chem. Phys. Lipids. 64 (1993) 129–142.
[198] P. Sukthankar, L.A. Avila, S.K. Whitaker, T. Iwamoto, A. Morgenstern, C. Apostolidis, K. Liu, R.P. Hanzlik, E. Dadachova, J.M. Tomich, Branched

amphiphilic peptide capsules: cellular uptake and retention of encapsulated solutes, Biochim. Biophys. Acta, Biomembr. 1838 (2014) 2296–2305.
[199] M.C. Morris, J. Depollier, J. Mery, F. Heitz, G. Divita, A peptide carrier for the delivery of biologically active proteins into mammalian cells, Nat. Biotechnol. 19 (2001) 1173–1176.
[200] S. Fawell, J. Seery, Y. Daikh, C. Moore, L.L. Chen, B. Pepinsky, J. Barsoum, Tat-mediated delivery of heterologous proteins into cells, Proc. Natl. Acad. Sci. U.S.A. 91 (1994) 664–668.
[201] B. Zhivotovsky, S. Orrenius, O.T. Brustugun, S.O. Doskeland, Injected cytochrome c induces apoptosis, Nature. 391 (1998) 449–450.
[202] J.S. Kim, J. Soucek, J. Matousek, R.T. Raines, Mechanism of ribonuclease cytotoxicity, J. Biol. Chem. 270 (1995) 31097–31102.
[203] J. Elgqvist, S. Frost, J.-P. Pouget, P. Albertsson, The potential and hurdles of targeted alpha therapy –, Clin. Trials Beyond. Front Oncol. 3 (2014) 1–9.
[204] O. Couturier, S. Supiot, M. Degraef-Mougin, A. Faivre-Chauvet, T. Carlier, J.F. Chatal, F. Davodeau, M. Cherel, Cancer radioimmunotherapy with alpha-emitting nuclides, Eur. J. Nucl. Med. Mol. Imaging 32 (2005) 601–614.
[205] M.R. McDevitt, R.D. Finn, G. Sgouros, D. Ma, D.A. Scheinberg, An 225Ac/213Bi generator system for therapeutic clinical applications: construction and operation, Appl. Radiat. Isot. 50 (1999) 895–904.
[206] A. Verma, O. Uzun, Y. Hu, Y. Hu, H.S. Han, N. Watson, S. Chen, D.J. Irvine, F. Stellacci, Surface-structure-regulated cell-membrane penetration by monolayer-protected nanoparticles, Nat. Mater 7 (2008) 588–595.
[207] S.E. Gratton, P.A. Ropp, P.D. Pohlhaus, J.C. Luft, V.J. Madden, M.E. Napier, J.M. DeSimone, The effect of particle design on cellular internalization pathways, Proc. Natl. Acad. Sci. U. S. A. 105 (2008) 11613–11618.